JNC TN9400 2002-077

Thermochemical investigation of sodium combustion

February 2003

OARAI ENGINEERING CENTER
JAPAN NUCLEAR CYCLE DEVELOPMENT INSTITUTE

JNC TN9400 2002-077
February, 2003

Thermochemical investigation of sodium combustion

Jintao HUANG*

Abstract

The present report summarizes the fundamental investigation on the thermochemical aspects of sodium combustion in case of sodium-leak incident of FBR. The main achievements obtained during the 3-years research since April 2000 can be classified as the following 6 categories,

(1) A high temperature mass spectrometer was developed to measure partial vapor pressures of the vapor species in a given system. By using this equipment, most of the possible sodium ferrates of Fe^{2+} and Fe^{3+} had been studied so that unknown properties of them were determined.

(2) Assessment of the thermodynamic data in Na-Fe-O system had been carried out so that a self-consistent data set for the main sodium ferrates $NaFeO_2$, Na_3FeO_3, Na_4FeO_3, Na_5FeO_4, $Na_8Fe_2O_7$, $Na_3Fe_5O_9$ as well as $Na_4Fe_6O_{11}$ was created.

(3) User databases for chemical equilibrium calculation code Thermo-Calc and MALT2 were made so that ternary phase diagrams of Na-Fe-O from room temperature to 1200K were constructed. Chemical potential diagrams as functions of P_{O2} and P_{Na} were given too. Thus, chemical stability of each phase was quantitatively determined.

(4) Further study in Na-Fe-O-H-C system had been made. The equilibrium states of sodium ferrates in H_2O/CO_2 environments were calculated by computer simulations. The results were displayed as functions pf P_{H2O} and P_{CO2} by using some predominance phase diagrams.

(5) A gas-inlet system was combined with the high temperature mass spectrometer. By introducing water vapor and/or carbon dioxide into the Knudsen cell, influence of water vapor and carbon dioxide on sodium ferrates was studied. By comparing the experimental data and the calculation results, the factors that affect the reaction process in thermodynamics as well as kinetics were discussed.

(6) The relationship between the possible corrosion types and the local environmental conditions was discussed based on the equilibrium calculation and the gas-inlet experiments.

Based on the present studies, main conclusions are as the following,

- The sodium ferrites, $NaFeO_2$, Na_3FeO_3, and Na_5FeO_4 could be formed in a wide range of temperature, oxygen potential and sodium pressure, while Na_4FeO_3 could be stable only at low oxygen potentials. $Na_8Fe_2O_7$ and $Na_3Fe_5O_9$ were found as the high temperature phases but $Na_4Fe_6O_{11}$ might be a metastable phase and tend to decompose to other sodium ferrites like $NaFeO_2$. Na_2FeO_2 does not exist and $Na_{31}Fe_8O_{29}$ reported in some literatures actually should be $Na_8Fe_2O_7$. Other higher order sodium iron oxides with $Fe^{+4,+5,+6}$ are unstable and will decompose to lower oxidation states.
- The equilibrium states in Na-Fe-O-H-C is greatly depends on the environmental conditions. Apart from temperature, oxygen potential and sodium pressure, the water vapor pressure and carbon dioxide pressure also have strong influence on behaviors of Na-Fe oxides in the Na-Fe-O-H-C system.
- Molten salt NaOH has high possibility to be formed in a wide range of temperature and gases conditions, which is one of the important factors in the so-called "Molten Salt Corrosion Mechanism" of sodium-leak incident of FBRs.
- It seems that the influence from CO_2 surpasses that of H_2O to dominate the chemical potential diagram, i.e., CO_2 may have stronger influence on equilibrium states in Na-Fe-O-H-C system than H_2O does. However, the kinetics of these chemical reactions may requires long time in hour-scale and sufficient mass transportation of water vapor and/or carbon dioxide from the surrounding environment to the reaction zone. The formation of NaOH is actually the dominant process instead of Na_2CO_3 in case of sodium ferrates in H_2O+CO_2 environments.
- The corrosion type at specific locations of reaction zone will depend on local environmental conditions. Molten Salts Corrosion would happen in the open interface where water vapor supply is adequate. On the other hand, the formation of Na-Fe complex oxides would be the main process in the closed inner areas that is isolated from the atmosphere by the reactants and products.

* Advanced Material Research Group, Advanced Technology Division,
O-arai Engineering Center

JNC TN9400 2002-077
２００３ 年 ２ 月

ナトリウム燃焼の化学熱力学に関する研究
-博士研究員詳細研究報告書-

黄 錦涛*

要 旨

本報告書は、高速増殖炉ナトリウム漏えい事故時におけるナトリウム燃焼にかかわる化学熱力学的評価に関する著者の研究成果の要約版である。2000 年 4 月からの 3 年間の研究成果は以下の 6 項目に分類される。

(1) 蒸気分圧を測定可能な高温質量分析システムを構築した。この分析装置を用いて、ほとんどの Fe^{2+}および Fe^{3+}の NaFe 複合酸化物について、熱力学特性に関する研究を実施した。

(2) 種種の NaFe 複合酸化物（$NaFeO_2$、Na_3FeO_3、Na_4FeO_3、Na_5FeO_4、$Na_8Fe_2O_7$、$Na_3Fe_5O_9$ および $Na_4Fe_6O_{11}$）について整合性のとれた熱力学データベースを構築するために、これら化合物の熱力学データの評価を行った。

(3) 室温から 1200K までの Na-Fe-O 系 3 元平衡状態図を作成するために、化学平衡計算コード Thermo-Calc および MALT2 用のユーザーデータベースを作成した。P_{O_2}および P_{Na}の関数とした化学ポテンシャル図も作成し、各相における化学的安定性を定量的に示した。

(4) さらに、研究を Na-Fe-O-H-C 系に発展させた。H_2O/CO_2 雰囲気における NaFe 複合酸化物の平衡状態をコンピュータシュミレーションにより計算した。その結果は、いくつかの平衡状態図を用いて P_{H_2O} と P_{CO_2} の関数として示した。

(5) 高温質量分析計にガス供給システムを付加した。水蒸気および／または CO_2 をクヌーセンセルに供給して、NaFe 複合酸化物の安定性に関する水蒸気および CO_2 の影響を調べた。実験データと計算結果の比較から、反応プロセスの考察を熱力学及び動力学見地から行った。

(6) 平衡計算とガス供給条件下における実験結果に基づいて、腐食機構と局所的な環境条件の関係を考察した。

これらの研究から得られた知見を以下に示す。

- $NaFeO_2$、Na_3FeO_3およびNa_5FeO_4は、広い温度範囲、酸素ポテンシャルそしてナトリウム分圧下で形成される。Na_4FeO_3は低酸素ポテンシャル下でのみ存在する。$Na_8Fe_2O_7$と$Na_3Fe_5O_9$は高温度域で存在する。$Na_4Fe_6O_{11}$は調査温度範囲内では安定に存在できず、$NaFeO_2$のような他のNaFe複合酸化物に分解する傾向がある。Na_2FeO_2は存在しえない。いくつか報告例のある$Na_{31}Fe_8O_{29}$は$Na_8Fe_2O_7$であった。他の高次鉄酸化物イオン$Fe^{+4,+5,+6}$からなるNaFe複合酸化物は安定に存在せず、低次鉄酸化物に分解すると考えられる。

- Na-Fe-O-H-C系の平衡状態はその環境条件に強く依存する。温度、酸素ポテンシャルおよびナトリウム分圧はさておき、水蒸気分圧とCO_2分圧もまた、Na-Fe-O-H-C中におけるNaFe複合酸化物のふるまいに強く影響する。

- 溶融塩型腐食発生因子の一つである$NaOH$は、広い温度範囲およびガス雰囲気で形成される高い可能性を示した。

- このNa-Fe-O-H-C系の中で、“平衡状態”として考えると、水蒸気分圧よりもCO_2分圧の方が安定性に強く影響する。しかしながら、これらの化学反応には数時間程度を必要とし、また周囲の環境から反応領域へのH_2Oおよび／またはCO_2の移行も影響する。実験からNa_2CO_3の形成より$NaOH$の形成の方が支配的なプロセスであることが分った。

- 腐食反応が進行する領域の腐食機構は、その局所的な環境条件に支配される。溶融塩型腐食は水蒸気が十分に供給されるような開放空間において進行する可能性がある。しかしながら、形成されるNaFe複合酸化物の化学状態は、その開放空間における環境条件よりもむしろ、漏えい堆積物中の環境条件に支配されるであろう。

* 要素技術開発部　新材料研究グループ

Contents

List of tables

List of figures

Thermochemical investigation of sodium combustion

1. Introduction

Sodium has been used as the coolant in Fast Breeder Reactors(FBR) for years because of its high power of heat transportation and many attractive advantages compared to other candidate coolants. On the other hand, the high chemical activity is considered as its main disadvantage. Thermochemical studies on sodium reaction with iron in accident conditions have caught enormous attentions in nuclear safety analysis as sodium-leak incident occurred from time to time especially during the testing operation periods in history. Thermodynamics plays an important role because it is a fundamental theory to estimate possible chemical reactions in various environmental conditions, evaluate possible consequences resulted form these reactions and help us to find better way to overcome problems.

Thermodynamics of Na-Fe-O is considered as one of the toughest topics in ternary systems. Since 1950s, a lot of research works have been done on sodium-iron oxides, such as $NaFeO_2$, Na_4FeO_3, Na_5FeO_4, Na_3FeO_3 and perhaps Na_2FeO_2. In 1951, Coughlin et al. probably were the first researchers who measured the heat capacity and entropy of $Na_2Fe_2O_4$[1](probably the same as $NaFeO_2$). In 1961, Koehler et al. studied heat of formation of α–$NaFeO_2$, β–$NaFeO_2$ and γ–$NaFeO_2$ by calorimetric measurement [2] while Watanabe reported crystal structure of β–$NaFeO_2$[3]. In 1984 Dai et al. tried to measure the standard Gibbs energy of $NaFeO_2$[4-5] but their results were suspected by themselves about 10 years later[6]. There is large disagreement even for the melting point and phase transformation temperatures, so Ono et al. reexamined the phase transformations between α–$NaFeO_2$ and β–$NaFeO_2$ at high temperatures by TG-DTA and DSC thermal analysis. They confirmed that phase transition from α–$NaFeO_2$ to β–$NaFeO_2$ is irreversible [7]. Till now, only thermodynamic data of $NaFeO_2$ was formally accepted by the Scientific Group Thermodata Europe(SGTE) among these ternary compounds[8-9]. Lindemer once evaluated thermodynamics for most of the Na-Fe-O compounds so that these evaluated data were widely used in 1980s[10]. However, Lindemer himself and some other researchers felt hard to explain some experimental results found later. A lot of efforts were paid to investigate these compounds. For example, Na_4FeO_3 had been studied extensively from 1970 to 1997 but careful evaluation is still in need to compare the results reported by different laboratories as summarized in Table 1. Attempts to understand more about these sodium-iron oxides

Table 1: Summary of $\Delta_f G°(Na_4FeO_3)$ J/mol = A + B×T (K)

Temperature	A	B	Error	Date	Ref.
400-1100K	-1160562.2	263.40	Not available	1993-1997 Thermo-Calc Database	Du, Dai Seetharaman Sweden [11]
371-904K	-1205503.3	347.28	Not available	1990 MALT2 database	Yokokawa Japan [12]
773-904K	-1168881.3	271.44	Not available	1989	Sridharan India [13]
723-873K	-1212202	351.10	±2100	1988	Bhat Germany [14]
298.15K	-1211000	337.644	Not available	1981	Lindemer USA [10]
700-1100K	-1215000	342.46	±12600	1977	Shaiu USA [15]

were ignited once again after the sodium-leaking incident at the Monju FBR in Japan, December 1995. One India group continued to work on this topic and investigated the thermodynamic stability of Na-Fe-O system[16-17]. On behalf of JNC, the Swedish Kungl Tekniska Högskolan(KTH) tried again to obtain thermodynamics data by using vapor pressure measurement method. Unfortunately, there are some serious concerns about their experimental results and conclusions.

In Na-Fe-O system, about 20 kinds of sodium ferrates [10, 18] have been reported in literatures (Fig. 1). Transition metal Fe possesses multi oxidation states of Fe^{+2}, Fe^{+3}, Fe^{+4},and Fe^{+6} in the solid state, so that it can form various complex compounds with alkaline metals. Those oxides with unusual high oxidation states such as iron valence over +4 are not stable and tend to decompose to its lower valence states [3]. Apart from Na_4FeO_3 with Fe^{+2} that is found at low oxygen potentials, sodium ferrites with Fe^{+3} $NaFeO_2$, Na_3FeO_3, Na_5FeO_4, $Na_8Fe_2O_7$, $Na_3Fe_5O_9$ as well as $Na_4Fe_6O_{11}$ are probably the most commonly found in nature. Though these Na-Fe oxides with Fe^{+2} and Fe^{+3} have been studied since 1950s[4-10], many discrepancies can be found in publications. So, it is really difficult for researchers to explain their experimental phenomena. Sometimes, even the basic Na-Fe-O phase diagrams published in literatures are quite debatable. The main reason could be attributed to the unreliable thermodynamic data for these compounds because most of the data were only theoretically estimated or evaluated from limited experiments.

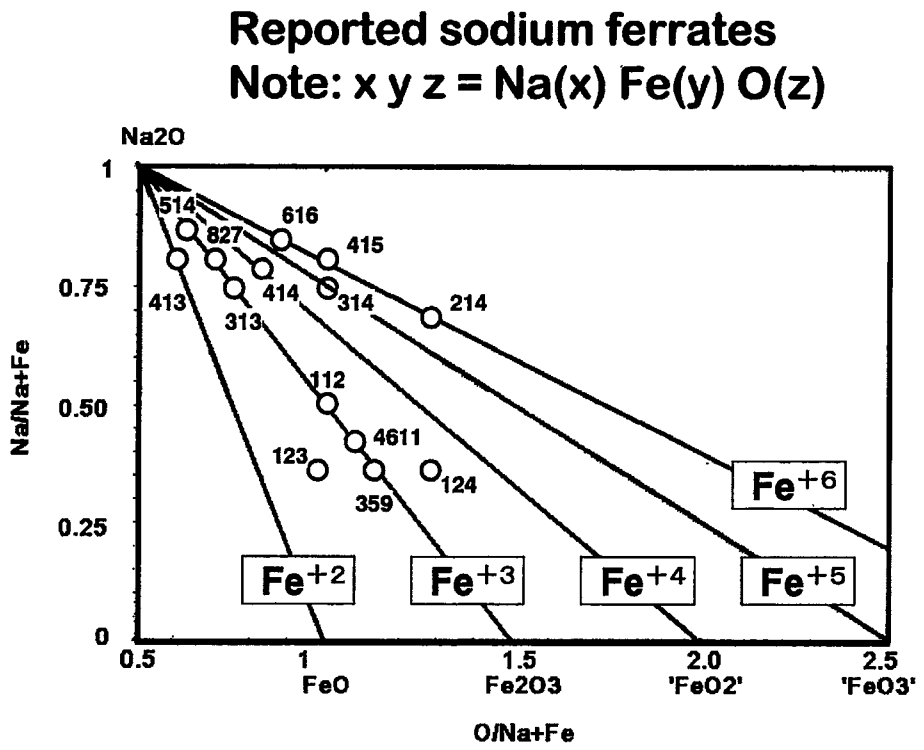

Fig. 1: Sodium ferrates reported in literatures

Understanding of the chemical behaviors of sodium ferrates in water vapor and carbon dioxide environments is essential to estimate the corrosion process of iron-based materials in sodium-leak incident of FBRs. Both computer simulation calculations at equilibrium states and the experimental measurements are necessary. Therefore, the following points are selected as the main research topics of the present study.

① Establish an effective way to obtain reliable thermodynamic properties of the main Na-Fe oxides.

As high temperature mass spectrometry is a well-known method to evaluate thermodynamic data of unknown compounds, a Knudsen effusion mass spectrometer(KEMS) was developed for this purpose as shown in Fig. 2. By measuring vapor pressure of the corresponding compound at high temperatures, unknown data such as the standard molar enthalpy of formation, the standard molar Gibbs energy of formation, must be determined.

② Careful assessment for the data obtained and the existing data in literatures

A self-consistent user database should be created so that further thermodynamic calculation by computer code such as Thermo-Calc and MALT2 could be carried out. Then, correct ternary phase diagram of the Na-Fe-O system and chemical potential diagram could be also made.

③ Investigation of their chemical stabilities at high temperatures.

For all the 7 kinds of sodium ferrates with Fe^{2+} and Fe^{3+}, possible phase transition, chemical reaction tendency at different conditions are of interests.

④ Computer simulation in Na-Fe-O-H-C system at high temperatures.

By using the thermodynamic data of the sodium ferrates evaluated in the previous studies, simulation calculations in Na-Fe-O-H-C system at high temperatures could be made. If chemical potential diagrams were constructed, the effects of H_2O and CO_2 on chemical behaviors of Na-Fe oxides could be understood.

⑤ Experimental confirmations on the environmental effects.

Further experiments should be done to investigate chemical behaviors of Na-Fe oxides in H_2O/CO_2 environments by introducing H_2 and CO_2 into the high temperature mass spectrometer. Experimental results should be compared with the calculated results in equilibrium states.

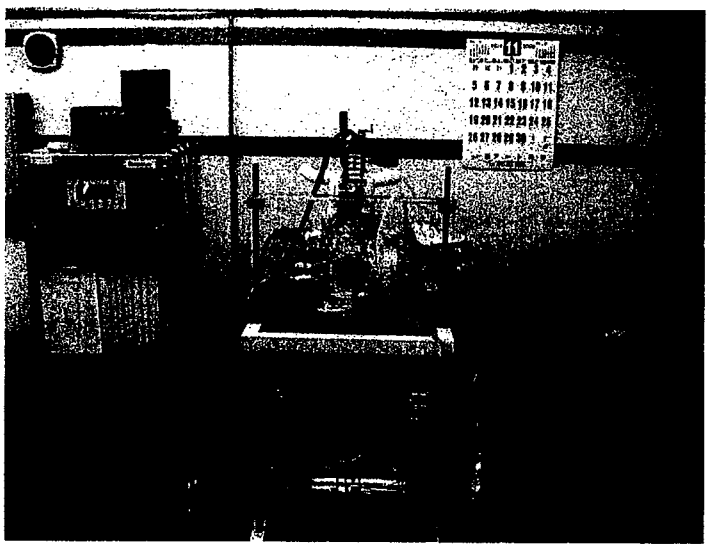

Fig. 2: The high temperature mass spectrometer developed in JNC

2. R&D of the high temperature mass spectrometer

In this section, principal and construction of the main equipment used for the thermodynamic measurement is briefly described. Details can be found in our previous reports[20-22].

2.1 The high temperature mass spectrometer

The principal of the high temperature mass spectrometer is well described in literatures[23-24]. In short, the partial vapor pressure P of each vapor species inside of the Knudsen cell can be measured by counting the corresponding ionized ion intensity I by a mass spectrometer as the following equation,

$$P = K\frac{I \times T}{\sigma} \quad \text{----------(1)}$$

where, T is the reaction temperature, σ is the electron ionization cross-section for the ion, K is the proportional factor that can be calibrated by standard reference.

The vapor pressure measurement system is comprised of a quadrupole mass spectrometer, a Knudsen vapor effusion cell(K-cell) as well as a vacuum chamber. Fig. 3 shows a schematic layout of the system. The system has sufficient capability for an ultimate pressure of 10^{-7} Pa. Experiments are always carried out in 10^{-6} Pa level even at high temperatures. High purity argon is used for purging the system. The quadrupole mass spectrometer "Microvision Plus LM70" is supplied by the Spectra Instruments. A faraday cup and a secondary electron multiplier are equipped within the analyzer to measure ion intensity. The secondly electron multiplier factor is calibrated by the faraday cup. A ThO_2-Ir filament is utilized in the ionization chamber to generate electrons with low impact energies. The electron impact energy can be set to be 9.8eV in order to get high counting and avoid possible cracks from sodium oxide vapor species.

The authors designed a K-cell with an orifice of 1±0.05 mm diameter as shown in Fig. 4. Special attention has been paid to choose a proper material to make the K-cell because sodium tends to react with cell materials. Mo and Pt had been used for K-cell materials in early mass spectrometric studies on sodium compounds. Compatible tests[25], however, showed that Na_2MoO_4 and $Na_2Mo_3O_6$ were formed when Mo was put together with $NaFeO_2$(s) around 1200K. Severe reaction between Mo and NaOH(liq) was also observed around 900K. So, Mo seems not a good choice for study of Na-Fe oxides. In contrast, Pt shows very good compatibility with sodium at high temperatures. No evidence of interactions between Pt and Na-containing substances was observed until

1400K. Meanwhile, it was found that sodium diffusion from the surface of Pt-cell to the outside caused a little high sodium background (mass=23). This effect could be greatly diminished when silver was coated on the inner surface of the Pt-cell cover[26]. Fortunately, no reactions between silver and sodium or iron were observed in the present measurements. Therefore, a Pt-cell with a silver-coated cover was employed to investigate vaporization behaviors of sodium iron complex oxides.

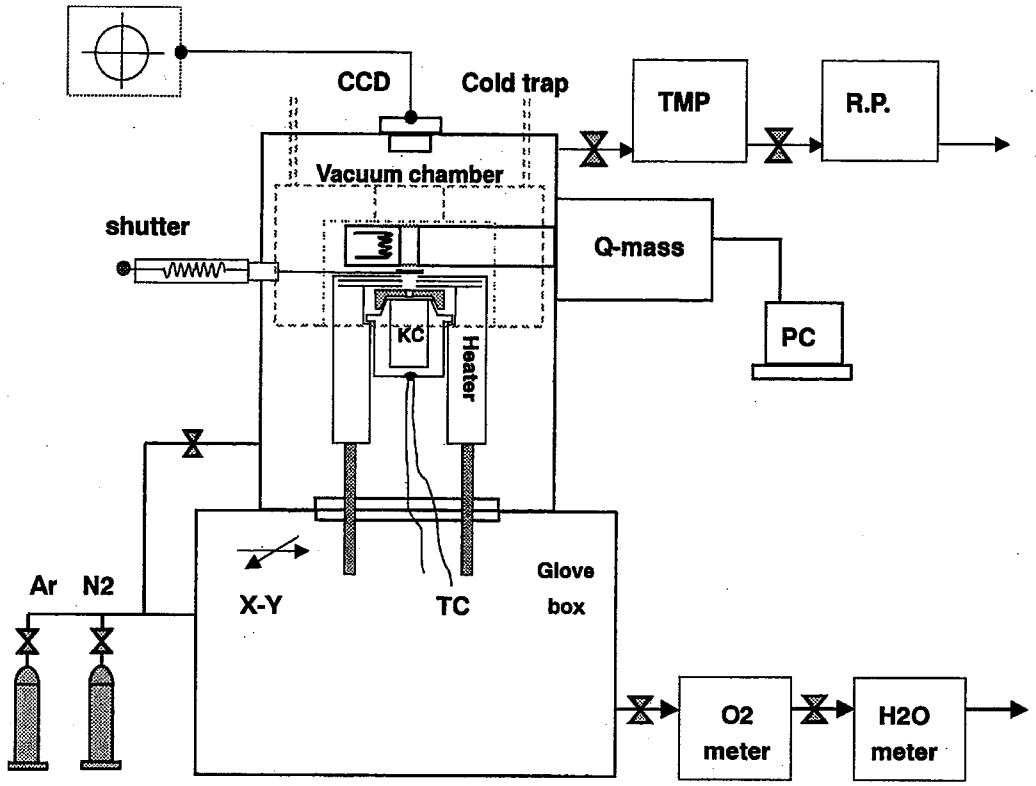

Fig. 3: Sketch of the KEMS

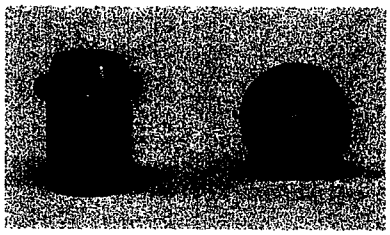

Fig. 4: Knudsen cell made of Pt

2.2 The gas-inlet system for the HTMS

To test the influence of water vapor and carbon dioxide on chemical behaviors of sodium ferrates, a gas-inlet high temperature mass spectrometer was built. As shown in Fig. 5-6, two fine tubes were connected to the Knudsen cell (KC) so that gases like H_2 and CO_2 could be introduced into the cell to react with Na-Fe oxides samples. Then, the partial vapor pressures of main vapor species in the system could be measured by the KEMS.

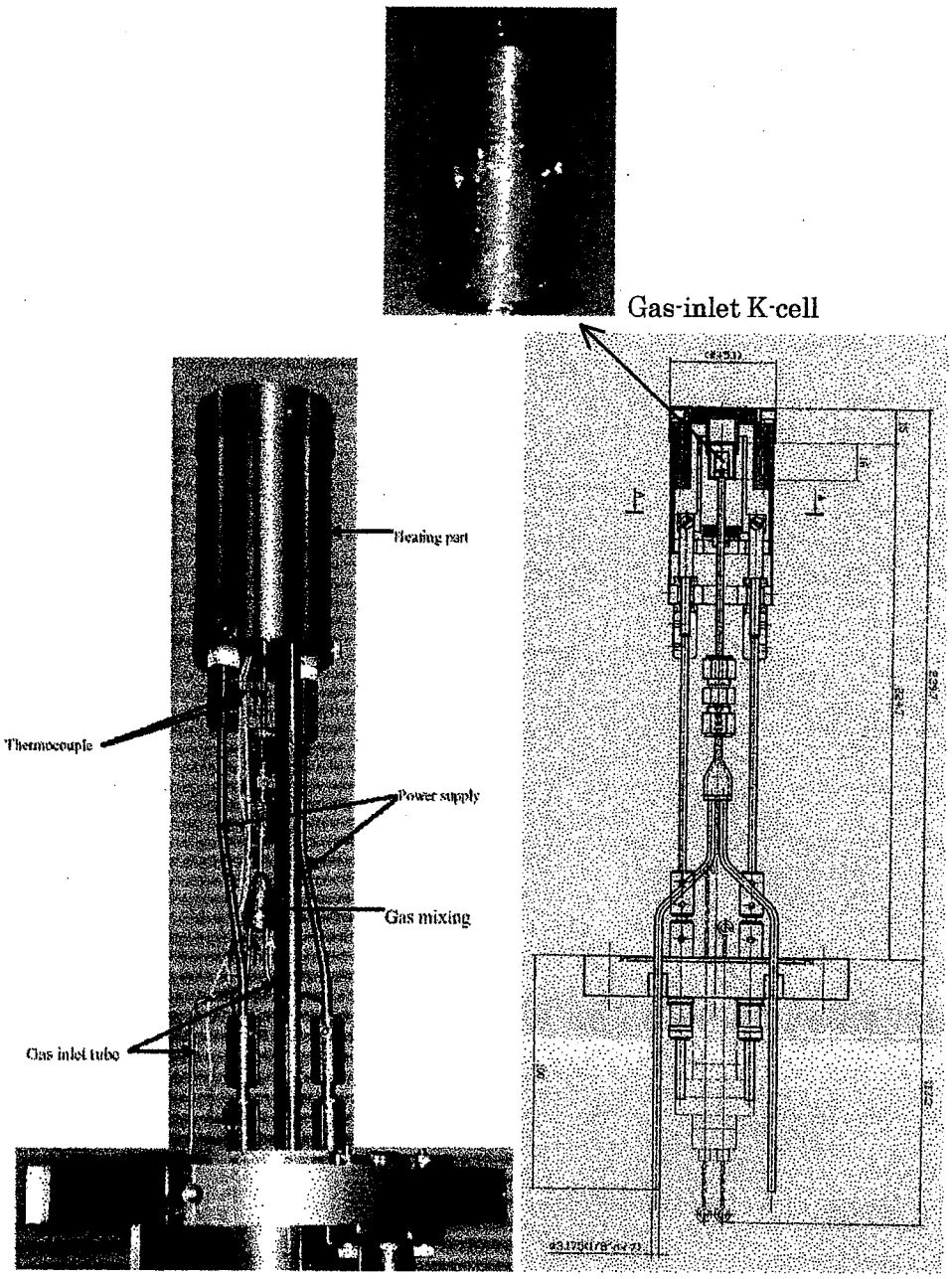

Fig. 5: Introduction of gases into the Knudsen cell

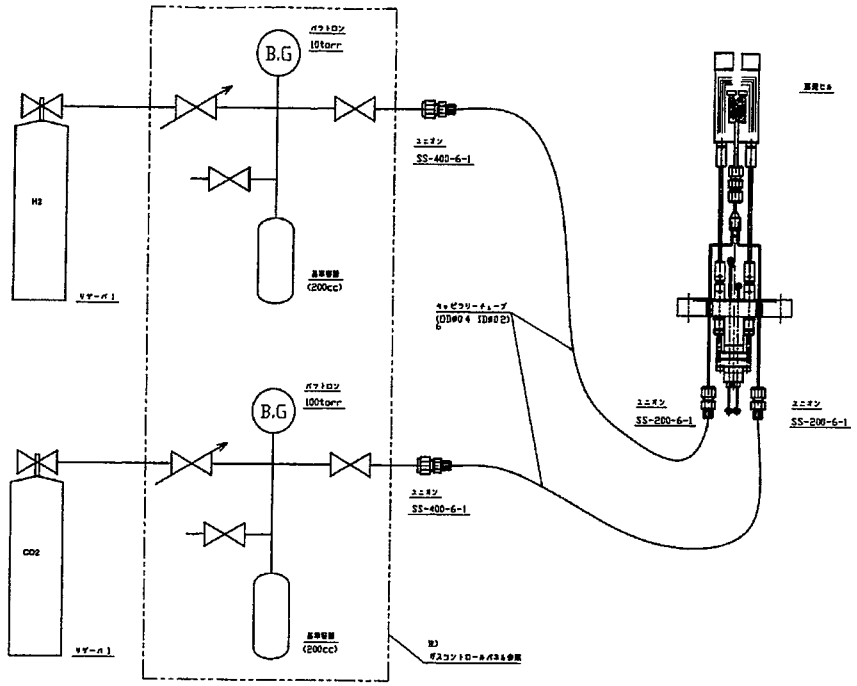

Fig. 6: The gas-inlet system

H_2 and CO_2 were chosen as the input gases to generate water vapor and carbon dioxide environment inside the KC reactor since they could produce H_2O and CO_2 environments as the following reaction.

$$H_2 + CO_2 = CO + H_2O \quad \cdots\cdots (2)$$

The amounts of H_2O and CO_2 produced inside the KC can be controlled by adjusting the input ratio of H_2/CO_2. Examples of environmental condition changes in KC by inputting H_2:CO_2=1:1 or 2:1 were shown in Fig. 7-8.

Oxygen potential in the system can be obtained either from reaction $H_2O=H_2+0.5O_2$ or $CO_2 = CO + 0.5O_2$. Example results at 800 K were listed in Table 2, where 3 inlet conditions CO_2:H_2=1:1, 1:2 and 2:1were tested. Some scatter in oxygen pressure could be found for the calculation for the two reactions, but generally correct order of oxygen potential was able to be determined.

Theoretic analysis and experiments were both carried out. Introducing CO_2+H_2 mixture gas is proved to be an effective way to generate H_2O+CO_2 atmosphere inside the reaction cell of high temperature mass spectrometer. So, the effects of H_2O+CO_2 atmosphere on stability of Na-Fe oxides can be examined this way.

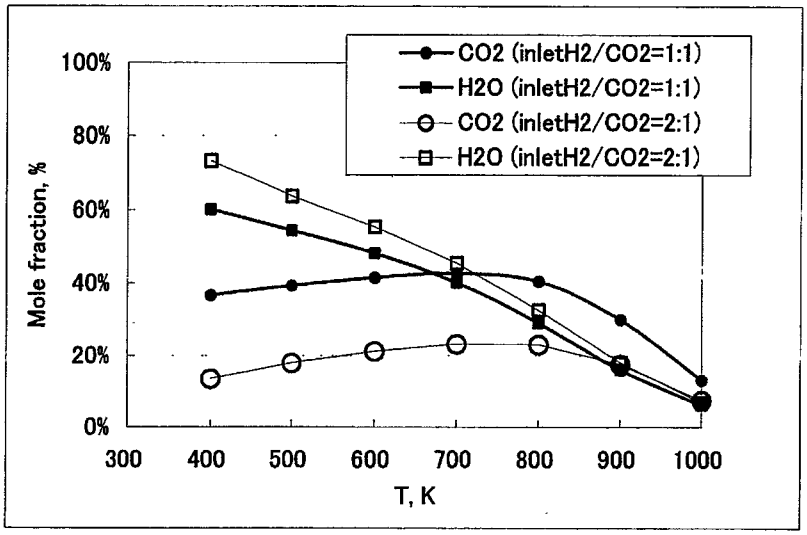

Fig. 7: Temperature dependency of environment changes in KC

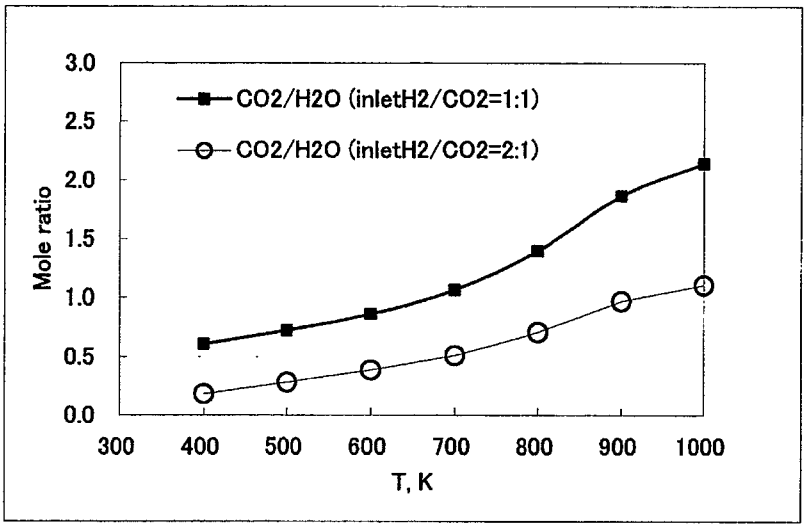

Fig. 8: Adjustment of CO_2/H_2O

Table 2: Oxygen pressure obtained from CO_2/CO and H_2O/H_2

	Experiment1	Experiment2	Experiment3
Inlet CO_2, torr	9.4	4.6	19.2
Inlet H_2, torr	9.3	9.1	9.0
Inlet ratio CO_2:H_2	1:1	1:2	2:1
Oxygen potential obtained from reaction $CO_2=CO+0.5O_2$			
$P(O_2)$/atm	3.6E-27	1.1E-27	2.4E-26
Oxygen potential obtained from reaction $H_2O=H_2+0.5O_2$			
$P(O_2)$/atm	2.0E-27	1.9E-27	3.9E-27
Equilibrium constant of $CO_2+H_2=CO+H_2O$			
Measured Kp	0.18	0.54	0.17
Kp (by JANAF)=0.237 while averaged Kp=0.29 (measured)			

2.3 Theoretic calculation of ionization cross-sections

As described in 2.1, ionization cross-section is required to calculate the partial vapor pressure for the vapor species of interest. Unfortunately, those data for sodium-containing molecules are seldom reported in literatures. So, a latest quantum mechanic model BEB was employed to calculate ionization cross-sections for these molecules. The model utilizes parameters of molecular orbital and ionization cross-section of a molecule could be estimated from the contributions from each molecular orbital. Readers should reference corresponding paper for the calculation details[27-28]. The result for the main sodium-containing molecules are shown in Fig. 9 and listed in Table 2. So, calculation of the partial vapor pressures of Na(g), Na2(g), NaO(g), Na_2O(g), NaOH(g) becomes possible as long as the ion intensity of these vapor species is measured by KEMS.

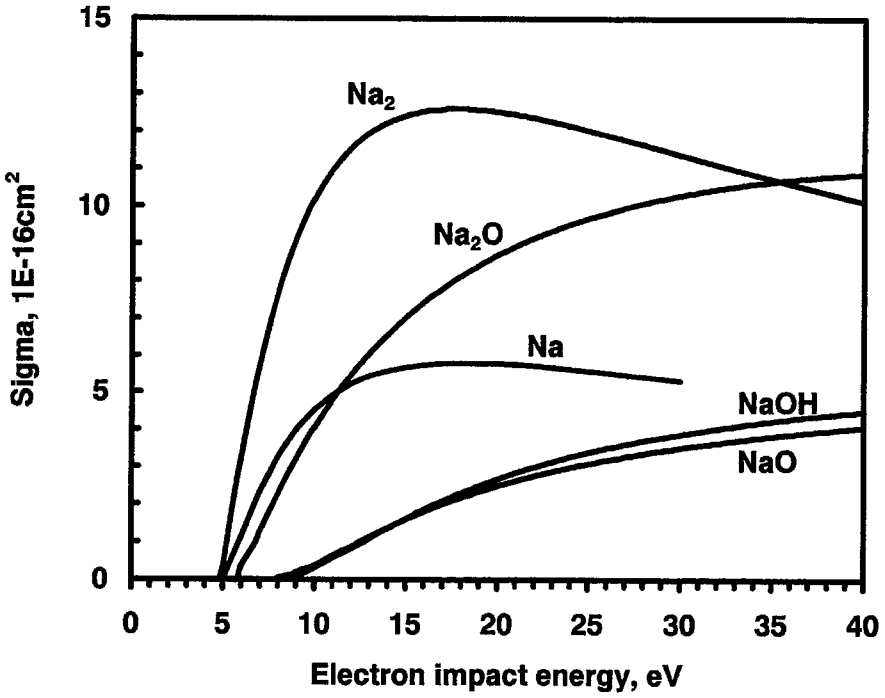

Fig. 9: Ionization cross-sections by BEB model

Table 3: The ionization cross-sections of sodium molecules (10^{-16} cm^2)

Impact Electron Energy T(eV)	σ(Na)	σ(NaO)	σ(NaOH)	σ(Na_2O)	σ(Na_2)
0-4	0.00	0.00	0.00	0.00	0.00
5	0.00	0.00	0.00	0.00	0.47
6	1.15	0.00	0.00	0.22	3.36
7	2.34	0.00	0.00	1.32	5.69
8	3.28	0.00	0.00	2.32	7.56
9	4.00	0.19	0.01	3.22	9.02
10	4.53	0.44	0.30	4.04	10.15
11	4.92	0.69	0.58	4.77	10.99
12	5.21	0.92	0.86	5.43	11.61
13	5.43	1.15	1.12	6.02	12.04
14	5.57	1.37	1.37	6.54	12.32
15	5.68	1.58	1.62	7.01	12.49
16	5.74	1.78	1.85	7.44	12.57
17	5.78	1.97	2.06	7.81	12.58
18	5.79	2.15	2.27	8.14	12.55
19	5.79	2.32	2.47	8.44	12.49
20	5.78	2.48	2.65	8.71	12.41
21	5.75	2.62	2.82	8.94	12.32
22	5.72	2.76	2.98	9.15	12.23
23	5.68	2.89	3.13	9.34	12.13
24	5.63	3.01	3.27	9.51	12.04
25	5.58	3.11	3.39	9.67	11.94
26	5.53	3.21	3.51	9.81	11.84
27	5.47	3.30	3.61	9.94	11.73
28	5.42	3.38	3.71	10.05	11.62
29	5.36	3.46	3.80	10.16	11.51
30	5.30	3.53	3.88	10.26	11.38

3. Thermodynamics of the Na-Fe-O system

3.1 Thermodynamic study by means of KEMS

Calibration of the KEMS was carried out first. Then, original thermodynamic data for Na_3FeO_3 and $Na_4Fe_6O_{11}$ were obtained by analyzing the chemical reactions

$Na_4FeO_3(s) = Na_4FeO_3(s) + Na(g)$ ----------(3)

$2Na_2CO_3(s)+3Fe_2O_3(s)= Na_4Fe_6O_{11}(s)+2CO_2(g)$ ----------(4)

3.1.1 Calibration

To make sure the reliability of the high temperature mass spectrometer, careful works were carried out before the investigation on Na-Fe oxides. Pressure calibration was made by using sodium as the standard substance[22,25]. Sodium (99.7%) was selected as the reference for this purpose because Na(g) is the main vapor species over Na-Fe oxides. So, the absolute partial vapor pressure of sodium can be obtained by the equation $P(Na)=K\times\{I\times T\}$, where I is the Na^+ ion intensity, T is the sample temperature. The proportional constant K is calibrated by the saturated vapor pressure of sodium given in literature[29].

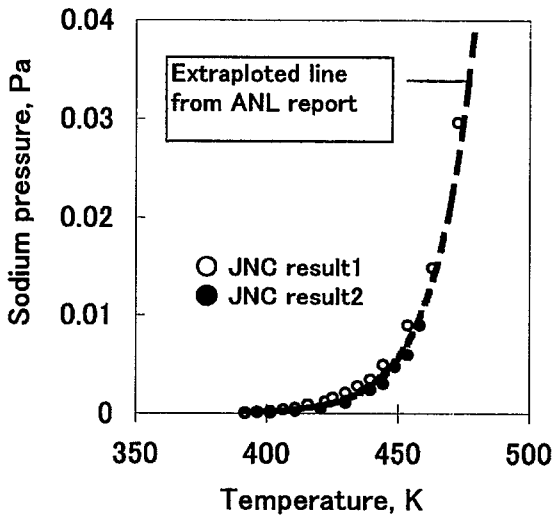

Fig. 10: Pressure-temperature relationship for Na(liq)=Na(g)

From the pressure-temperature relationship obtained over Na(liq)=Na(g) as shown in Fig 10, the standard enthalpy of formation of Na(g) was calculated by the 3rd law treatment as $\Delta_f H°(298.15K)$ = 107.6±0.8 kJ mol^{-1}. This agrees well with the 107.3 kJ mol^{-1} given by the NIST-JANAF Thermodynamic Tables[30]. A comparison with data reported by other laboratories all over the world is given in Table 4. It shows the good

precision of the high temperature mass spectrometer used in the present study so that the reliability of the measurements in the present laboratory can be guaranteed.

Table 4: Comparison of $\Delta_f H°$(Na(g), 298.15K) reported in literature

$\Delta_f H°$(298.15K)	Source
107.3±0.70	NIST-JANAF, CODATA Recommended, 1998
107.6±0.8	Huang, JNC
107.52±0.68	Haycock & Lamplough
107.37±0.60	Rodebush & Devries
107.99±0.60	Thiele
107.38±0.70	Kis Tiakowsky
107.18±0.95	Makansi et al.
107.26±0.78	Shpil rain & Belova
107.60±1.35	Sowa
107.68±1.33	Stone et al.
107.85±0.80	Achener & Jouthas
107.44±0.60	Vinogradov
107.47±1.00	Bohdansky
107.36±1.22	Schins et al.
Note: Data from Ref.30, page 1641.	

3.1.2 Thermodynamic analysis of Na_3FeO_3 by means of KEMS

Vaporization behaviors of Na_4FeO_3(s) were studied from 590 to 717 K by the vapor pressure measurement system. New data of the Gibbs energy of formation of Na_3FeO_3(s) was obtained based on the experimental results. Na_4FeO_3(s) sample was synthesized from its corresponding component oxides Na_2O(s) and FeO(s). The source materials were prepared by mixing purified Na_2O(s) (99.4%) and FeO(s) (99.9%) powders with molar ratio of 2:1. Then the whole sample was sealed in a stainless steel container in a glove box in which oxygen and water vapor concentrations were strictly controlled as less than 10ppm. Finally, the specimen had been sintered at 873 K for 100 hours.

$$2Na_2O(s) + FeO(s) = Na_4FeO_3(s) \text{----------} (5)$$

A X-ray powder diffraction(XRD) identification showed that the prepared sample was almost pure Na_4FeO_3(s) according to JCPDS file No. 34-0891. Prepared sample Na_4FeO_3(s) was continuously stored in a glove box before it was transferred into the K-cell for vapor pressure measurements. Sample installation was carried out in another glove box attached to the high temperature mass spectrometer.

Two separate measurements on Na_4FeO_3(s) were made by the high temperature mass spectrometer. The first specimen was measured over a period of 4 hours in the temperature range of 590-717K. After the vapor pressure measurement, a mixture of Na_4FeO_3(s) and Na_3FeO_3(s) was identified by XRD analysis. A rough comparison indicated a molar ratio of Na_4FeO_3 : $Na_3FeO_3 \approx 9 : 1$. The second Na_4FeO_3(s) specimen was evaporated for about 30 hours in the high temperature mass spectrometer. It resulted in a complete decomposition from Na_4FeO_3(s) into Na_3FeO_3(s). Though one small peak of NaOH was also identified by XRD, it should be attributed to possible moisture absorption from the environment when the sample was analyzed by XRD. Thus, the following reaction is assumed to have occurred inside the K-cell,

$$Na_4FeO_3(s) = Na_3FeO_3(s) + Na(gas) \quad \text{----------(6)}$$

The temperature dependence of sodium vapor pressure was determined by measuring Na^+ intensity as temperature was changed step by step. Sodium vapor species was able to be detected over about 550K and was found as the main vapor species over Na_4FeO_3(s). Dimmer Na_2(g) was also able to be identified but its intensity was only 3-4 orders of magnitude lower than that of the monomer. No other vapor species such as NaO(g) and Na_2O(g) were observed due to the detection limit. The temperature dependence of sodium pressure over Na_4FeO_3(s) was plotted in Fig. 11. The data obtained from the two specimens show consistent results. Based on the present experimental results, the partial vapor pressure of sodium over Na_4FeO_3(s) in the temperature range from 590 to 717 K can be expressed as,

$$\ln P_{Na} = 24.376 - 17749/T \quad \text{----------(7)}$$

Thermodynamic functions related to the decomposition reaction (6) were calculated from the 25 experimental points as listed in Table 5. Gibbs energy change of the reaction was obtained.

$$\Delta_r G^\circ(T) = (148522.2 \pm 2753.8) - (108.29 \pm 4.18) \times T \quad (590\text{–}717\ \text{K}) \quad \text{----------(8)}$$

Table 5: Thermodynamic functions for $Na_4FeO_3(s)= Na_3FeO_3(s)+Na(gas)$

No.	T/K	P_{Na}/Pa	$\Delta rG°(T)$/ J mol^{-1}	Kp
1	590.6	4.10E-03	83575	4.05E-08
2	606.4	8.09E-03	82397	7.99E-08
3	622.3	1.69E-02	80736	1.67E-07
4	638.2	3.58E-02	78816	3.54E-07
5	654.0	6.25E-02	77752	6.17E-07
6	664.6	8.91E-02	77051	8.79E-07
7	669.9	1.09E-01	76554	1.07E-06
8	675.2	1.27E-01	76281	1.25E-06
9	685.8	2.40E-01	73861	2.37E-06
10	696.4	3.53E-01	72751	3.49E-06
11	701.6	4.31E-01	72150	4.25E-06
12	701.6	5.31E-01	70931	5.24E-06
13	706.9	6.00E-01	70746	5.92E-06
14	712.2	6.57E-01	70734	6.49E-06
15	717.5	7.27E-01	70661	7.17E-06
16	590.6	3.68E-03	84112	3.63E-08
17	601.1	6.13E-03	83064	6.05E-08
18	611.7	1.01E-02	81999	9.95E-08
19	622.3	1.49E-02	81397	1.47E-07
20	632.9	2.19E-02	80742	2.17E-07
21	643.5	3.35E-02	79834	3.30E-07
22	654.0	5.19E-02	78763	5.12E-07
23	664.6	8.50E-02	77306	8.39E-07
24	675.2	1.20E-01	76601	1.18E-06
25	685.8	1.80E-01	75495	1.78E-06

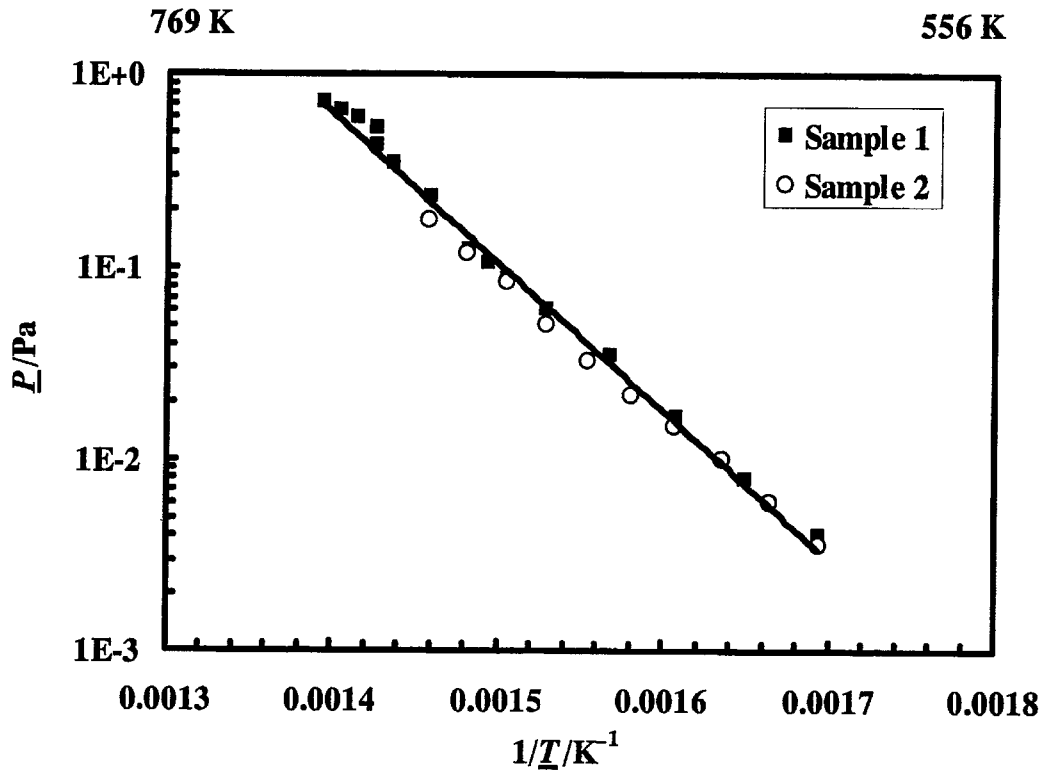

Fig. 11: Temperature dependence of partial vapor pressure of sodium over Na_4FeO_3

Then, $\Delta_f G°(Na_3FeO_3)$ can be derived as the following,

$$\Delta_f G°(Na_3FeO_3) = \Delta_r G°(T) - \Delta_f G°(Na, gas) + \Delta_f G°(Na_4FeO_3). \quad \cdots\cdots(9)$$

From SGTE database given by Thermo-Calc[31], the Gibbs energy of formation of Na(gas) can be expressed as $\Delta_f G°(Na, gas)=104949-95.53\times T$. Thermodynamic data of $Na_4FeO_3(s)$ have been experimentally measured and theoretically estimated in publications [11-15]. The Gibbs energy of formation given by Bhat and Borgstede [14] was employed in the present study, i.e.,

$$\Delta_f G°(Na_4FeO_3) = -1212202 + 351.10\times T. \quad \cdots\cdots(10)$$

Finally, the Gibbs energy of formation of $Na_3FeO_3(s)$ was determined as,

$$\Delta_f G°(Na_3FeO_3) = -1168629 + 338.34\times T \quad (298 < T < 720K) \quad \cdots\cdots(11)$$

The precision of $\Delta_f G°(Na_3FeO_3)$ expressed here is depending on the source data of

$\Delta_f G°(Na_4FeO_3)$. The error in $\Delta_f G°(Na_3FeO_3)$ is estimated as about ±7 kJ mol^{-1} since an error of ±2100 J mol^{-1} in $\Delta_f G°(Na_4FeO_3)$ was given by Bhat and Borgstede.

Up to date, experimentally measured results of $\Delta_f G°(Na_3FeO_3)$ have been seldom reported in publications. Other thermodynamic data, such as heat capacities, enthalpy increments and Gibbs energy functions of Na_3FeO_3 and Na_4FeO_3 are not available either. So, it is unable to evaluate $\Delta_f H°(298)$ of Na_3FeO_3 by the 3rd law method for the time being. A comparison with existing theoretic estimations, however, is possible and significant. For example, $\Delta_f G°(Na_3FeO_3)$ is supplied by a Japanese thermodynamic database MALT2[32] in which thermodynamic data of $Na_3FeO_3(s)$ were estimated from very limited experimental data as well as those of its corresponding component oxides. As shown in Fig. 12, the Gibbs energy of formation of $Na_3FeO_3(s)$ given by the MALT2 is considerably close to the present result.

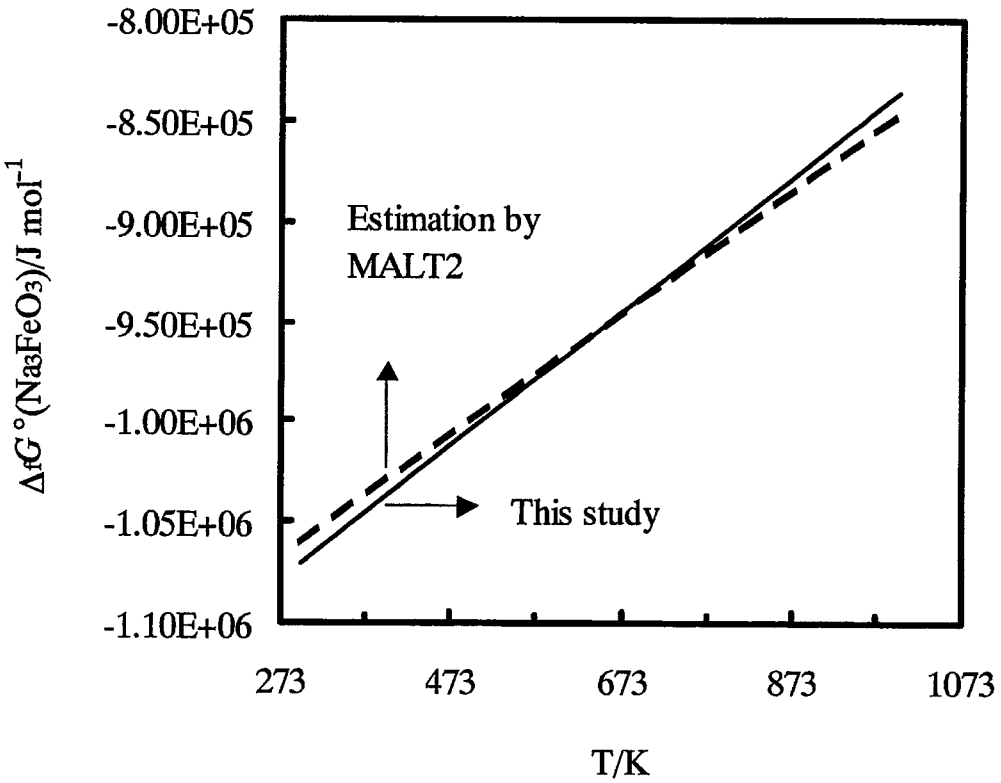

Fig. 12: Data comparison of $\Delta_f G°(Na_3FeO_3)$/J mol^{-1}

3.1.3 Thermodynamic analysis of $Na_4Fe_6O_{11}$ by means of KEMS

It is reported that single phase $Na_4Fe_6O_{11}$ could be produced by heating sodium carbonate Na_2CO_3 with ferric oxide Fe_2O_3 (2:3)[33-35]. Thus, Na_2CO_3 and Fe_2O_3 were

employed as the stating materials for vapor pressure measurements. Fine powders of Na_2CO_3 (99.999%, RARE METALLIC Co., Ltd.) and Fe_2O_3 (99.999%, SOEKAWA CHEMICALS) were mixed and pressed into plate with molar ration of 2:3 in Ar atmosphere. Then the sample was installed in the Knudsen cell made of Pt. The orifice used in the experiment was in diameter of 1 mm.

Baking process was carried out around 627 K for over 24 hours until the absorption gas impurities such as water vapor and carbon dioxide in the sample were deduced to the background level. The vapor pressure measurements were conducted from 918 to 1023 K. CO_2 was found as the main vapor species during our experimental measurement. Some evidence of Na, NaOH and CO were also detected in the experiments but their intensities were observed close to the background level. The electron impact energy was set to be 20 eV to obtain large ion intensity. Pressure calibration was made by using pure silver as the standard reference. So, the pressure of CO_2 is calculated as the following equations:

$$p(CO_2)=K*[I(CO_2^+)*T]/\sigma(CO_2) \quad \text{----------(12)}$$

$$K=p(Ag)*\sigma(Ag)/[I(Ag+)*T] \quad \text{----------(13)}$$

where, p is the absolute vapor pressure, I is the ion intensity measured by the mass spectrometer, and σ is the electron impact ionization cross-section. The electron ionization cross-sections of CO_2 and Ag at 20 eV were taken from literatures[36-37], i.e., $\sigma(CO_2)/M^2 = 0.508 \times 10^{-20}$ and $\sigma(Ag)/M^2 = 4.50 \times 10^{-20}$.

After the mass spectrometric measurement, a black colored product was found together with the starting materials Na_2CO_3 in white and Fe_2O_3 in red. The sample was analyzed by X-ray powder diffraction. It is found that the peaks from the product of present experiment were consistent with the X-ray diffraction pattern of $Na_4Fe_6O_{11}$ reported by Hua et al[35] and Watanabe et al[34]. Therefore, it is assumed that the following reaction occurred in the Knudsen cell during the mass spectrometric tests.

$$2Na_2CO_3+3Fe_2O_3=Na_4Fe_6O_{11}+2CO_2(gas) \quad \text{----------(14)}$$

Thus, thermodynamic data of $Na_4Fe_6O_{11}$ can be evaluated from the experimental values of vapor pressure of CO_2 as properties of the left substances in the reaction are well known.

Table 6: Partial CO_2 pressure over the mixture of $2Na_2CO_3+3Fe_2O_3$

	Experiment 1		Experiment 2	
No.	T/K	$p(CO_2)$/Pa	T/K	$p(CO_2)$/Pa
1	923	0.46393	918.15	0.43650
2	933	0.66301	928.15	0.51630
3	943	0.85807	938.15	0.76762
4	953	1.13145	948.15	1.04258
5	963	1.66909	958.15	1.54938
6	973	2.27667	968.15	2.19178
7	983	2.98157	978.15	2.84710
8	993	3.87245	988.15	4.02670
9	1003	4.95450	998.15	5.48782
10	1013	7.11080	1008.15	7.30346
11	1008	5.50332	1018.15	9.21988
12	998	4.32438	913.15	0.36029
13	989	3.08548	923.15	0.47769
14	978	2.20362	933.15	0.65187
15	968	1.59387	943.15	0.91508
16	958	1.11248	953.15	1.29469
17	948	0.98586	963.15	1.74436
18	938	0.55276	973.15	2.39193
19	928	0.43428	983.15	3.05243
20	918	0.34209	993.15	4.11131
21			1003.15	5.45043
22			1013.15	7.79841
23			1023.15	9.92695

The partial vapor pressures of CO_2 over the mixture of $2Na_2CO_3+3Fe_2O_3$ obtained by the KEMS were given in Table 6 in detail. The first sample of about (50 mg) was measured for about 6 hours around 970 K and the second sample (200 mg) for about 15 hours. Both samples showed very close slope of $\ln P(CO_2)$ against $1000/T$ as shown in Fig. 13. The differences in the absolute pressures for the two samples should be attributed to some minor variation of the sealing performance of the Pt-made Knudsen cell which could be caused during sample handling. The temperature dependences of CO_2 partial pressure can be expressed as the following equation:

$$\ln\{p(CO_2)/\mathrm{Pa}\}=(29.4385\pm0.3244)+(-29015.4\pm313.55)\times K/T, (918\text{-}1023K) \quad \cdots\cdots(15)$$

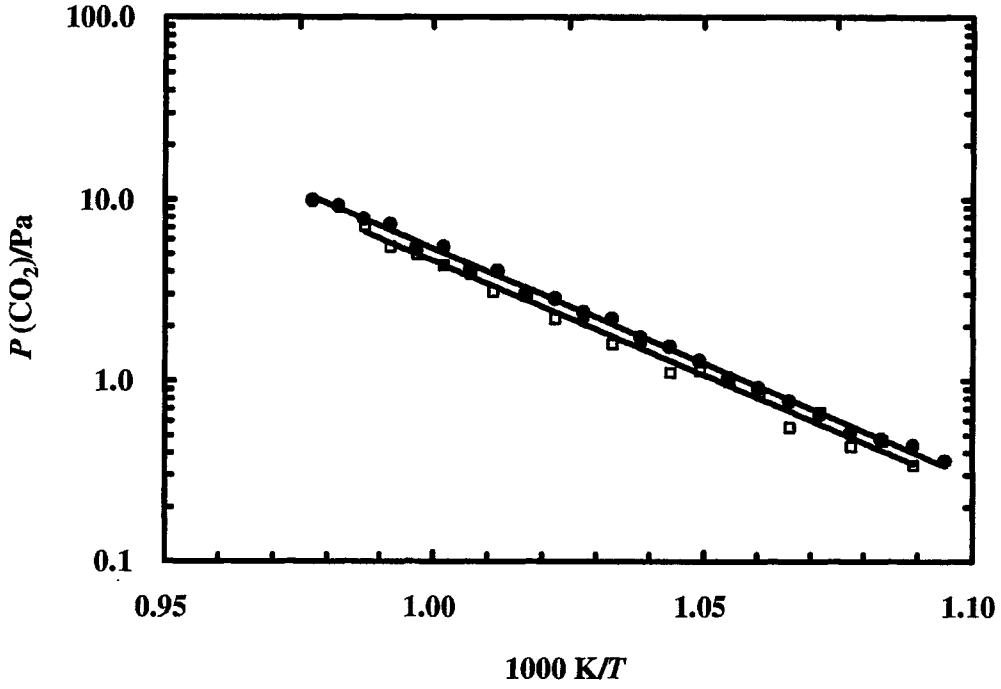

Fig. 13: Pressure-temperature dependence of CO_2 over $2Na_2CO_3+3Fe_2O_3$.
□, experiment 1; ●, experiment 2; ——, least squares fitting.

The enthalpy change of reaction(14) at the average temperature of the measurements was calculated as $\Delta_r H°_m(970\ K)\ /kJ\cdot mol^{-1} = 241.2\pm2.6$.

By using thermodynamic data of Na_2CO_3, Fe_2O_3 and CO_2(gas) given in the SGTE database, thermodynamic treatments by the 2nd law and the 3rd law have been made, respectively. Standard molar enthalpy of formation of $Na_4Fe_6O_{11}$ at 298.15 K was determined as:

$$\Delta_f H°_m(Na_4Fe_6O_{11}, 298.15K)\ /J\cdot mol^{-1} = -3569.54 \pm 3.95. \quad \text{(16)}$$

The standard molar Gibbs energy of formation of $Na_4Fe_6O_{11}$ was derived as:

$$\Delta_f G°_m(Na_4Fe_6O_{11})/J\cdot mol^{-1}=(-3716839\pm2274.55)+(1200.16\pm2.35)\times T/K. \quad \text{(17)}$$

$\Delta_f G°_m(Na_4Fe_6O_{11}, 298.15\ K)$ could be estimated by employing the following equation:

$$\Delta_f G°_m(Na_4Fe_6O_{11}, 298.15\ K) = \Delta_f H°_m(298.15\ K) - 298.15\times\Delta_f S°_m(298.15\ K) \quad \text{(18)}$$

where, $\Delta_f S°_m$(298.15 K) is the standard entropy of formation from its component elements in their standard states.

$S°_m(Na_4Fe_6O_{11}, 298.15\ K)$ = 442 $J \cdot mol^{-1} \cdot K^{-1}$ estimated by Lindemer et al.[10] was utilized for this calculation. Thus, $\Delta_f G°_m(Na_4Fe_6O_{11}, 298.15\ K)$ is recommended as $-3255.3 \pm 12.4\ kJ \cdot mol^{-1}$. Heat capacity $Cp(Na_4Fe_6O_{11})$/ $J \cdot mol^{-1} \cdot K^{-1}$ was estimated from its corresponding component binary oxides. The Gibbs energy function *gef*(*T*) was calculated using the following equation:

$$gef_m(T) = [G°_m - H°_m(298.15\ K)]/T = -S°_m(T) + [H°_m(T) - H°_m(298.15\ K)]/T \quad \text{----------(19)}$$

It is noticed that $\Delta_f H°_m(Na_4Fe_6O_{11}, 298.15K)$ of $Na_4Fe_6O_{11}$ obtained by the 2nd law method in the present study is quite close to the $-3665\ kJ \cdot mol^{-1} \cdot K^{-1}$ given by Lindemer by the same treatment[10]. However, his estimation was mainly based on Knight and Philips' early experiment and could only provide a rough result. According to the more precise measurements in the present study, more positive value in Gibbs free energy of $Na_4Fe_6O_{11}$ is evaluated. Therefore, the high temperature form sodium ferrite $Na_4Fe_6O_{11}$ should be considered as a metastable phase if it appeared at relatively low temperatures.

3.2 Thermodynamic database of the Na-Fe-O system

3.2.1 Binary and ternary systems

Thermodynamic basis of equilibrium calculation and the construction of phase diagram by the Thermo-Calc can be found in literature [31] as well as the User's guide. Present study employed TERN-module to create the ternary phase diagrams of the Na-Fe-O system. POLY-module was used to generate the potential diagram. The SSUB database provided by SGTE is employed as the main database for the calculation. A user database was built up for the calculation. Thermodynamic data source and assessment of literatures and experimental results are given as the following.

① Na-O system

A schematic binary Na-O phase diagram can be found in literature [38]. The three binary oxides in the system, Na_2O(s), Na_2O_2(s) and NaO_2(s), were taken into account in the present calculation but no solutions were included for lack of necessary data.

② Fe-O system

This system is extensively investigated so that original data given in the SSUB database were utilized for the calculation, in which the three well known solid solutions, Hematite, Magnetite and Wustite were included. Further discussion in this part is no longer necessary.

③ Na-Fe system

No further treatment was done for this binary system because no compounds were found and only very limited solutions were reported.

④ $NaFeO_2$(s)

Data assessed by SGTE was used. Thermodynamic data of $NaFeO_2$(s) used for the present calculation are given in detail in Table 9-15 together with other ternary Na-Fe oxides. The Gibbs energy of formation of $NaFeO_2$(s) can be expressed as,

$$\Delta_f G^\circ(Na_4FeO_3) = -701849.4 + 204.19 \times T \quad \text{----------(20)}$$

⑤ Na_4FeO_3(s)

This compound has been studied so many times that thermodynamic evaluation are possible. Among the available data of Na_4FeO_3(s), Bhat and Borgstede's result [14] seems more reliable because their result agrees quite well with experimental data given by Gross [39] and Shaiu[15]. Therefore, the following expression is employed in the present study.

$$\Delta_f G^\circ(Na_4FeO_3) = -1212202 + 351.10 \times T \quad \text{----------(21)}$$

Since experimental data, such as heat capacities, enthalpy increments and Gibbs energy functions of Na_4FeO_3(s) are not available, estimated data have to be used. So, Lindemer's estimation of entropy $S^\circ(298)=208.9$ J $mol^{-1}K^{-1}$ was employed. Heat capacity $Cp(T)$ given by MALT2 database[32] was employed that was estimated from those of its component oxides. $\Delta_f H^\circ(298)$ was calculated according to the following formula.

$$\Delta_f H°(298) = \Delta_f G°(298) + T\Delta_f S°(298) \quad \cdots\cdots (22)$$

Thermal analysis on this compound by DSC carried out in the present laboratory shows that the melting point is around 1008±15 K. No other phase transitions were found up to its melting point. Property of its liquid phase is not determined so the whole calculation was done below its melting point.

⑥ $Na_3FeO_3(s)$

Experimental measurement on this compound was very scarce. In the present study, vaporization behavior of $Na_4FeO_3(s)$ was thermodynamically studied from 590 to 717K by means of high temperature mass spectrometry. It was found that $Na_4FeO_3(s)$ decomposed into $Na_3FeO_3(s)$ and released sodium vapor. The temperature dependence of partial vapor pressure of sodium over $Na_4FeO_3(s)$ was measured so that the Gibbs energy of formation of $Na_3FeO_3(s)$ was evaluated as as expressed in the following,

$$\Delta_f G°(Na_3FeO_3) = -1168629 + 338.34 \times T \quad \cdots\cdots (23)$$

The expression should be valid until about 1000 K because no phase transition was observed till 1033K by DSC and XRD analysis. Similar treatments were made to estimate $S°(298)$, $Cp(T)$ and $\Delta_f H°(298)$ of $Na_3FeO_3(s)$ as expressed above.

⑦ $Na_5FeO_4(s)$

Thermal analysis in the present laboratory shows that there are no phase transitions for this compound from room temperature to 1000 K. Up to date, experimentally measured results of $\Delta_f G°(Na_5FeO_4)$ have been seldom reported in publications. Thermodynamic data for this compound, $\Delta_f H°(298) = -1596$ kJ mol^{-1}, $S°(298) = 246.3$ J mol^{-1} K^{-1} were employed according to Lindemer's estimation while heat capacity was estimated in the similar way as described above.

$$\Delta_f G°(Na_5FeO_4) = -1602430 + 467.3 \times T \quad \cdots\cdots (24)$$

⑧ $Na_8Fe_2O_7$

The standard enthalpy of formation was given as $\Delta_f H°(Na_8Fe_2O_7) = -2746.0$ kJ mol^{-1} by Stuve et al. in 1971 [40]. Lindemer et al[10] estimated the entropy of $Na_8Fe_2O_7$ as about $S°(298) = 438.1$ J mol^{-1} K^{-1}. So, $\Delta_f H°(Na_8Fe_2O_7)$ was able to be calculated by eq.(9), i.e. $\Delta_f H°(298) = -2524.3$ kJ mol^{-1}. Its heat capacity was roughly calculated from

those of Na_3FeO_3(s) and Na_5FeO_4(s).

$$\Delta_f G°(Na_8Fe_2O_7) = -2754068 + 771.86 \times T \quad \cdots\cdots (25)$$

⑨ $Na_4Fe_6O_{11}$

Thermodynamic data of $Na_4Fe_6O_{11}$ was evaluated based on the reaction $2Na_2CO_3+3Fe_2O_3=Na_4Fe_6O_{11}+2CO_2$. Standard molar enthalpy of formation of $Na_4Fe_6O_{11}$ at 298.15 K, $\Delta_f H°_m(Na_4Fe_6O_{11}, 298.15K)$, was determined as -3569.54 ± 3.95 kJ·mol^{-1}. The standard molar Gibbs energy of formation at 298.15 K, $\Delta_f G°_m(Na_4Fe_6O_{11}, 298.15\ K)$, was evaluated as -3255.3 ± 12.4 kJ·mol^{-1}. $S°_m(Na_4Fe_6O_{11}, 298.15\ K) = 442$ J·mol^{-1}·K^{-1} estimated by Lindemer et al.(1) was utilized. Thus, $\Delta_f G°_m(Na_4Fe_6O_{11}, 298.15\ K)$ is recommended as -3255.3 ± 12.4 kJ·mol^{-1}. Heat capacity $Cp(Na_4Fe_6O_{11})$/ J·mol^{-1}·K^{-1} was estimated from its corresponding component binary oxides.

$$\Delta_f G°(Na_8Fe_2O_7) = -2754068 + 771.86 \times T \quad \cdots\cdots (26)$$

⑩ $Na_3Fe_5O_9$

Kale and Srikanth[41] obtained the Gibbs energy of formation of $Na_3Fe_5O_9$ by using solid-state electrochemical cells where $\Delta G°(Na_3Fe_5O_9)$ from solid Na_2O and α–Fe_2O_3 was derived as the following. So, the standard Gibbs energy of formation of $Na_3Fe_5O_9$ was estimated as $\Delta_f G°(Na_3Fe_5O_9) = -2646.0$ kJ/mol while the standard enthalpy of formation of $Na_3Fe_5O_9$ was evaluated as $\Delta_f H°(Na_3Fe_5O_9) = -2904.4$ kJ/mol. The standard Gibbs energy of $Na_3Fe_5O_9$ was reevaluated by using the entropy $S°(298) = 346$ J/molK estimated by Lindemer[10], heat capacity $Cp(T) = 422.93 + 7.819 \times 10^2\ T - 5.907 \times 10^6 / T^2$ estimated from its corresponding simple oxides as given by MALT2.

$$\Delta_f G°(Na_4Fe_6O_{11}) = -2914665 + 876.68 \times T \quad \cdots\cdots (27)$$

⑪ Na_2FeO_2(s) and other higher order oxides

It is reasonable to exclude Na_2FeO_2(s) from the present calculation since experimental attempts to produce this phase failed and theoretic analysis suspected its stability [6,16,17]. Though some higher order Na-Fe oxides, such as $Na_{10}Fe_{16}O_{29}$ and $Na_{34}Fe_8O_{29}$ had been reported[10], they were observed neither in the present laboratory nor in Sridharan's[13,16,17]. So, these compounds were not considered in the present calculation too.

3.2.2 Thermodynamic table for the ternary Na-Fe oxides

Based on the thermodynamic evaluation in the Na-Fe-O system, a user database was created both for the Thermo-calc computer code and also for the MALT2 computer code. It is found that both codes can provide good phase diagrams or chemical potential diagrams if the same thermodynamic data were used for the equilibrium calculation.

The user data file for the Thermo-Calc is given in Table 7.

Table 7: The JNC user data for the Thermo-Calc

	$G(T) = g0 + g1 \times T + g2 \times T \times \ln(T) + g3 \times T^2 + g4 \times T^3 + g5/T$, J mol^{-1}					
	g0	g1	g2	g3	g4	g5
$NaFeO_2$	-723394.6	455.160	-80.55	-0.00666	0	0
Na_3FeO_3	-65606.3	1071.530	-181.69	-0.01670	0	1483500
Na_4FeO_3	-76071.2	1244.166	-212.49	-0.01916	0	1642000
Na_5FeO_4	-1691381.1	1551.917	-262.60	-0.02409	0	2228000
$Na_9Fe_5O_9$	-149384.0	2543.152	-422.93	-0.03910	0	2953500
$Na_4Fe_6O_{11}$	-185215.5	3135.930	-523.70	-0.04839	0	3693000
$Na_8Fe_2O_7$	-2906986.6	2603.706	-444.30	-0.04078	0	3711000

The user data file for the MALT2 windows version is given in Table 8.

Considering the common habits of readers, the JANAF format was employed to display the whole thermodynamic table for these compounds. Data of heat capacity, entropy, enthalpy increment, the Gibbs energy function, the standard Gibbs energy of formation and the standard enthalpy of formation were listed from room temperature to 1500K. By using MALT2 computer code, the complete thermodynamic tables for the 7 ternary Na-Fe oxides were given in Table 9-15.

Table 8: The JNC user data file for the MALT2 windows version

```
      UserData: By Dr. Huang
*
Na3FeO3                                    s   s   -1162.6   -1068.6   172.0      1
 S313                          c    181.69    33.39     -29.67    0.0       0.0
                               298.15    1500.0    0.0
*
; Changed :02/08/29 10:19:04
Na4FeO3                                    sl  sl  -1206.1   -1107.5   208.9      2
 s                             c    212.49    38.31     -32.84    0.0       0.0
                               298.15    1008.0    0.0       mp
 l                             liq  247.874  0.0       0.0       0.0       0.0
                               1008.0    1500.0    0.0
*
; Changed :02/08/29 11:15:26
Na3Fe5O9                                   s   s   -2904.4   -2646.0   346.0      1
                               c    422.93    78.19     -59.07    0.0       0.0
                               298.15    1500.0    0.0       bp
*
; Changed :02/08/29 11:10:56
NaFeO2                                     s   s   -698.787   -640.52   88.3       1
 s                             s    80.55     13.31     0.0       0.0       0.0
                               298.15    1500.0    0.0
*
; Changed :02/09/10 10:12:30
Na8Fe2O7                                   s   s   -2746.00   -2524.30  438.1      1
                               c    444.3     81.56     -74.22    0.0       0.0
                               298.15    1500.0    0.0
*
; Changed :02/12/02 16:42:27
Na4Fe6O11                                  s   s   -3569.54   -3255.26  442.0      1
                               c    523.7     96.78     -73.86    0.0       0.0
                               298.15    1500.0    0.0
```

Table 9: Thermodynamic table of $NaFeO_2$

T	*Cp*	*S*°	*H*°-*H*°(298)	*gef*	$\Delta_f H°$	$\Delta_f G°$
K	J/K·mol	J/K·mol	kJ/mol	J/K·mol	kJ/mol	kJ/mol
298.15	84.518	88.3	0	-88.3	-698.787	-640.52
300	84.543	88.823	0.156	-88.302	-698.784	-640.159
371	85.488	106.878	6.192	-90.187	-698.79	-626.305
371	[Na:mp] 2.6					
371	85.488	106.878	6.192	-90.187	-701.388	-626.305
400	85.874	113.327	8.677	-91.634	-701.478	-620.437
500	87.205	132.632	17.331	-97.97	-701.848	-600.152
600	88.536	148.649	26.118	-105.119	-702.325	-579.782
700	89.867	162.397	35.038	-112.342	-702.95	-559.322
800	91.198	174.484	44.092	-119.369	-703.796	-538.758
900	92.529	185.302	53.278	-126.104	-704.95	-518.071
1000	93.86	195.12	62.597	-132.522	-706.509	-497.234
1042	94.419	198.993	66.551	-135.124	-707.31	-488.431
1042	[Fe:mtp] 0.75					
1042	94.419	198.993	66.551	-135.124	-708.06	-488.431
1100	95.191	204.128	72.05	-138.628	-709.14	-476.178
1170.44	96.129	210.065	78.788	-142.75	-710.042	-461.234
1170.44	[Na:] 97.25					
1170.44	96.129	210.065	78.788	-142.75	-807.288	-461.234
1184	96.309	211.174	80.093	-143.528	-807.311	-457.225
1184	[Fe:tp] 0.9					
1184	96.309	211.174	80.093	-143.528	-808.211	-457.225
1200	96.522	212.468	81.636	-144.438	-808.106	-452.484
1300	97.853	220.246	91.354	-149.974	-807.438	-422.881
1400	99.184	227.547	101.206	-155.257	-806.749	-393.33
1500	100.515	234.435	111.191	-160.308	-806.037	-363.829

Table 10: Thermodynamic table of Na_3FeO_3

T	*Cp*	*S*°	*H*°-*H*°(298)	*gef*	$\Delta_f H°$	$\Delta_f G°$
K	J/K·mol	J/K·mol	kJ/mol	J/K·mol	kJ/mol	kJ/mol
298.15	158.268	172	0	−172	−1162.6	−1068.6
300	158.74	172.98	0.293	−172.003	−1162.59	−1068.02
371	172.522	208.24	12.096	−175.637	−1162.08	−1045.6
371	[Na:mp] 2.6					
371	172.522	208.24	12.096	−175.637	−1169.87	−1045.6
400	176.502	221.377	17.158	−178.481	−1169.65	−1035.87
500	186.517	261.921	35.346	−191.228	−1168.24	−1002.48
600	193.482	296.573	54.363	−205.968	−1166.12	−969.449
700	199.008	326.826	73.996	−221.118	−1163.6	−936.807
800	203.766	353.717	94.139	−236.043	−1160.86	−904.544
900	208.078	377.969	114.734	−250.487	−1158.08	−872.629
1000	212.113	400.103	135.746	−264.358	−1155.43	−841.017
1042	213.75	408.864	144.689	−270.007	−1154.4	−827.819
1042	[Fe:mtp] 0.75					
1042	213.75	408.864	144.689	−270.007	−1155.15	−827.819
1100	215.967	420.502	157.151	−277.637	−1153.64	−809.619
1170.44	218.605	433.988	172.457	−286.645	−1151.32	−787.637
1170.44	[Na:] 97.25					
1170.44	218.605	433.988	172.457	−286.645	−1443.06	−787.637
1184	219.107	436.509	175.425	−288.347	−1442.23	−780.044
1184	[Fe:tp] 0.9					
1184	219.107	436.509	175.425	−288.347	−1443.13	−780.044
1200	219.698	439.454	178.935	−290.342	−1442	−771.087
1300	223.341	457.184	201.088	−302.501	−1434.84	−715.437
1400	226.922	473.866	223.601	−314.151	−1427.45	−660.347
1500	230.456	489.643	246.47	−325.33	−1419.82	−605.793

Table 11: Thermodynamic table of Na_5FeO_4

T	*Cp*	*S°*	*H°-H°(298)*	*gef*	$\Delta_f H°$	$\Delta_f G°$
K	J/K·mol	J/K·mol	kJ/mol	J/K·mol	kJ/mol	kJ/mol
298.15	226.859	246.3	0	-246.3	-1596	-1462.7
300	227.564	247.705	0.42	-246.304	-1596	-1461.87
371	248.118	298.343	17.371	-251.52	-1595.58	-1430.17
371	[Na:mp] 2.6					
371	248.118	298.343	17.371	-251.52	-1608.57	-1430.17
400	254.038	317.244	24.655	-255.606	-1608.4	-1416.23
500	268.88	375.649	50.857	-273.936	-1606.71	-1368.36
600	279.143	425.624	78.283	-295.153	-1603.84	-1320.94
700	287.244	469.282	106.615	-316.976	-1600.17	-1274.07
800	294.193	508.102	135.694	-338.485	-1595.99	-1227.77
900	300.472	543.12	165.431	-359.308	-1591.55	-1182
1000	306.335	575.084	195.774	-379.31	-1587.06	-1136.74
1042	308.71	587.736	208.69	-387.458	-1585.21	-1117.87
1042	[Fe:mtp] 0.75					
1042	308.71	587.736	208.69	-387.458	-1585.96	-1117.87
1100	311.926	604.545	226.689	-398.464	-1583.29	-1091.88
1170.44	315.75	624.024	248.796	-411.458	-1579.52	-1060.53
1170.44	[Na:] 97.25					
1170.44	315.75	624.024	248.796	-411.458	-2065.75	-1060.53
1184	316.477	627.665	253.083	-413.913	-2064.4	-1048.89
1184	[Fe:tp] 0.9					
1184	316.477	627.665	253.083	-413.913	-2065.3	-1048.89
1200	317.332	631.919	258.153	-416.791	-2063.57	-1035.17
1300	322.608	657.528	290.151	-434.335	-2052.5	-949.914
1400	327.789	681.626	322.672	-451.146	-2041.06	-865.527
1500	332.9	704.416	355.707	-467.278	-2029.24	-781.97

Table 12: Thermodynamic table of Na_4FeO_3

T	*Cp*	*S*°	*H*°-*H*°(298)	*gef*	$\Delta_f H°$	$\Delta_f G°$
K	J/K·mol	J/K·mol	kJ/mol	J/K·mol	kJ/mol	kJ/mol
298.15	186.969	208.9	0	-208.9	-1206.1	-1107.5
300	187.494	210.058	0.346	-208.904	-1206.09	-1106.89
371	202.844	251.6	14.251	-213.188	-1205.58	-1083.46
371	[Na: mp]			2.6		
371	202.844	251.6	14.251	-213.188	-1215.97	-1083.46
400	207.289	267.037	20.2	-216.538	-1215.78	-1073.11
500	218.509	314.589	41.531	-231.528	-1214.33	-1037.58
600	226.354	355.155	63.792	-248.835	-1212	-1002.44
700	232.605	390.531	86.749	-266.604	-1209.11	-967.729
800	238.007	421.951	110.285	-284.095	-1205.89	-933.46
900	242.915	450.271	134.334	-301.011	-1202.55	-899.604
1000	247.516	476.105	158.858	-317.247	-1199.27	-866.119
1008	247.874	478.079	160.839	-318.516	-1199.01	-863.455
1008	[Na4FeO3:bp]					
1008	247.874	478.079	160.839	-318.516	-1199.01	-863.455
1042	247.874	486.302	169.267	-323.857	-1197.98	-852.154
1042	[Fe:mtp]			0.75		
1042	247.874	486.302	169.267	-323.857	-1198.73	-852.154
1100	247.874	499.728	183.644	-332.78	-1196.98	-832.908
1170.44	247.874	515.114	201.104	-343.295	-1194.57	-809.668
1170.44	[Na:]			97.25		
1170.44	247.874	515.114	201.104	-343.295	-1583.55	-809.668
1184	247.874	517.969	204.465	-345.279	-1582.6	-800.707
1184	[Fe:tp]			0.9		
1184	247.874	517.969	204.465	-345.279	-1583.5	-800.707
1200	247.874	521.296	208.431	-347.604	-1582.25	-790.137
1300	247.874	541.137	233.219	-361.738	-1574.54	-724.44
1400	247.874	559.506	258.006	-375.216	-1566.94	-659.332
1500	247.874	576.608	282.793	-388.079	-1559.48	-594.763

Table 13: Thermodynamic table of $Na_8Fe_2O_7$

T	*Cp*	*S*°	*H*°-*H*°(298)	*gef*	$\Delta_f H°$	$\Delta_f G°$
K	J/K·mol	J/K·mol	kJ/mol	J/K·mol	kJ/mol	kJ/mol
298.15	385.124	438.1	0	-438.1	-2746	-2524.3
300	386.301	440.486	0.714	-438.107	-2745.99	-2522.92
371	420.636	526.383	29.467	-446.957	-2745.06	-2470.22
371	[Na:mp] 2.6					
371	420.636	526.383	29.467	-446.957	-2765.85	-2470.22
400	430.537	558.419	41.813	-453.887	-2765.46	-2447.12
500	455.392	657.368	86.202	-484.964	-2762.35	-2367.83
600	472.619	741.994	132.644	-520.921	-2757.36	-2289.37
700	486.245	815.905	180.608	-557.892	-2751.17	-2211.84
800	497.951	881.613	229.83	-594.326	-2744.25	-2135.25
900	508.541	940.884	280.162	-629.593	-2737.03	-2059.55
1000	518.438	994.981	331.515	-663.465	-2729.89	-1984.65
1042	522.45	1016.392	353.374	-677.262	-2727.01	-1953.41
1042	[Fe:mtp] 0.75					
1042	522.45	1016.392	353.374	-677.262	-2728.51	-1953.41
1100	527.882	1044.839	383.834	-695.899	-2724.33	-1910.37
1170.44	534.343	1077.804	421.247	-717.899	-2718.25	-1858.43
1170.44	[Na:] 97.25					
1170.44	534.343	1077.804	421.247	-717.899	-3496.22	-1858.43
1184	535.573	1083.966	428.501	-722.056	-3494.03	-1839.47
1184	[Fe:tp] 0.9					
1184	535.573	1083.966	428.501	-722.056	-3495.83	-1839.47
1200	537.018	1091.164	437.082	-726.93	-3492.97	-1817.11
1300	545.936	1134.502	491.231	-756.632	-3474.75	-1678.18
1400	554.697	1175.282	546.264	-785.093	-3455.91	-1540.68
1500	563.341	1213.847	602.166	-812.403	-3436.48	-1404.55

Table 14: Thermodynamic table of $Na_3Fe_5O_9$

T	*Cp*	*S*°	*H*°-*H*°(298)	*gef*	$\Delta_f H°$	$\Delta_f G°$
K	J/K·mol	J/K·mol	kJ/mol	J/K·mol	kJ/mol	kJ/mol
298.15	379.792	346	0	-346	-2904.4	-2646
300	380.754	348.352	0.704	-346.007	-2904.33	-2644.4
371	409.022	432.384	28.826	-354.686	-2901.17	-2583.22
371	[Na:mp] 2.6					
371	409.022	432.384	28.826	-354.686	-2908.97	-2583.22
400	417.287	463.483	40.811	-361.457	-2907.58	-2557.81
500	438.397	559.031	83.669	-391.694	-2902.1	-2470.98
600	453.436	640.35	128.293	-426.528	-2896.15	-2385.31
700	465.608	711.187	174.262	-462.241	-2890.36	-2300.64
800	476.252	774.068	221.365	-497.362	-2885.25	-2216.76
900	486.008	830.732	269.483	-531.306	-2881.35	-2133.44
1000	495.213	882.418	318.548	-563.87	-2879.19	-2050.48
1042	498.964	902.869	339.426	-577.125	-2878.93	-2015.68
1042	[Fe:mtp] 0.75					
1042	498.964	902.869	339.426	-577.125	-2882.68	-2015.68
1100	504.057	930.034	368.514	-595.022	-2882.12	-1967.43
1170.44	510.135	961.508	404.234	-616.139	-2879.25	-1908.93
1170.44	[Na:] 97.25					
1170.44	510.135	961.508	404.234	-616.139	-3170.98	-1908.93
1184	511.293	967.391	411.16	-620.128	-3169.89	-1894.32
1184	[Fe:tp] 0.9					
1184	511.293	967.391	411.16	-620.128	-3174.39	-1894.32
1200	512.656	974.263	419.351	-624.804	-3172.44	-1877.03
1300	521.082	1015.631	471.039	-653.293	-3160.06	-1769.58
1400	529.382	1054.552	523.563	-680.578	-3147.4	-1663.1
1500	537.59	1091.356	576.913	-706.747	-3134.44	-1557.53

Table 15: Thermodynamic table of $Na_4Fe_6O_{11}$

T K	$C_{p,m}(T)$ J·mol^{-1}·K^{-1}	$S°_m(T)$ J·mol^{-1}·K^{-1}	$H°_m-H°_m$(298.15 K) kJ·mol^{-1}	$gef(T)$ J·mol^{-1}·K^{-1}	$\Delta_f H°_m(T/K)$ kJ·mol^{-1}	$\Delta_f G°_m(T/K)$ kJ·mol^{-1}
298.15	469.467	442.000	0.000	-442.000	-3569.540	-3255.260
300	470.667	444.908	0.870	-442.009	-3569.456	-3253.310
371	505.944	548.821	35.646	-452.740	-3565.687	-3178.885
371	Na: melting point 2.60					
371	505.944	548.821	35.646	-452.740	-3576.079	-3178.885
400	516.249	587.293	50.472	-461.113	-3574.430	-3147.898
500	542.546	705.522	103.504	-498.514	-3567.800	-3042.002
600	561.251	806.168	158.735	-541.610	-3560.508	-2937.519
700	576.373	893.853	215.637	-585.800	-3553.321	-2834.258
800	589.583	971.695	273.947	-629.262	-3546.903	-2731.982
900	601.683	1041.845	333.517	-671.270	-3541.896	-2630.432
1000	613.094	1105.834	394.261	-711.573	-3538.940	-2529.336
1042	617.742	1131.153	420.108	-727.978	-3538.464	-2486.944
1042	Fe: melting point 0.75					
1042	617.742	1131.153	420.108	-727.978	-3542.964	-2486.944
1100	624.054	1164.785	456.121	-750.130	-3542.052	-2428.176
1170	631.584	1203.752	500.345	-776.267	-3538.319	-2356.950
1170	[Na:] 97.25					
1170	631.584	1203.752	500.345	-776.267	-3927.303	-2356.950
1184	633.019	1211.035	508.919	-781.204	-3925.889	-2338.765
1184	[Fe:tp] 0.90					
1184	633.019	1211.035	508.919	-781.204	-3931.289	-2338.765
1200	634.707	1219.543	519.061	-786.992	-3928.824	-2317.261
1300	645.144	1270.760	583.055	-822.256	-3913.194	-2183.593
1400	655.424	1318.948	648.085	-856.030	-3897.183	-2051.143
1500	665.587	1364.514	714.136	-888.424	-3880.795	-1919.851

3.3 Phase diagrams of the Na-Fe-O system

By means of Thermo-Calc code, new chemical potential diagram and ternary Na-Fe-O phase diagram were constructed up to about 1200K. Isothermal sections of the ternary phase diagram were illustrated. Stability of the ternary oxides was quantitatively discussed.

3.3.1 Na-Fe-O ternary phase diagrams

Many pioneers have studied ternary phase diagrams of the Na-Fe-O system but there still exist discrepancies. Early phase diagram study on the Na-Fe-O system had been done by Dai et al.[4-5] and Knights and Phillips[42]. Some isothermal phase diagrams of FeO(s)-Na_2O(s), FeO(s)-$Na_2Fe_2O_4$(s) and Fe_3O_4(s)-$Na_2Fe_2O_4$(s) were given. Lindemer et al. constructed ternary Na-Fe-O phase diagram and Ellingham diagram in which Na_2FeO_2(s), $Na_8Fe_2O_7$(s), $Na_3Fe_5O_9$(s) as well as $Na_4Fe_6O_{11}$(s), were included by using estimated thermodynamic data. Their work correctly predicted the formation of Na(l)-Fe(s)-Na_4FeO_3(s) at high temperatures though stability of some ternary oxides involved had not been confirmed[10]. Partial phase diagram at low oxygen potentials and oxygen-sodium potential diagram at 853K were presented by Seetharaman et al. Possibility of formation of Na_2FeO_2(s) was ruled out by them by thermodynamic analysis[6]. Sridharan et al. did extensive experiments by thermal analysis, solid-state reactions etc... so that partial phase diagram over 773K was deduced[16-17]. However, large discrepancy can be found among the available phase diagrams mentioned above. For example, Sridharan et al.[16] suggested that there exist two-phase lines Na_4FeO_3(s)-Na_3FeO_3(s) and Na_3FeO_3(s)-$NaFeO_2$(s) in 500-650°C while Seetharaman et al.[6] reported Na_4FeO_3(s)-$NaFeO_2$(s) and Na_2O(s)-$NaFeO_2$(s) two-phase lines within the same temperature zone. Therefore, vapor pressure measurements on some Na-Fe oxides and DSC thermal analysis were done in the present laboratory. Thermodynamic functions of Na_3FeO_3 and Na_4FeO_3 were evaluated once again. By using the JNCA user database, new ternary phase diagrams in the Na-Fe-O system were constructed from room temperature to 1200K by the Thermo-Calc code as shown in Fig. 14-20.

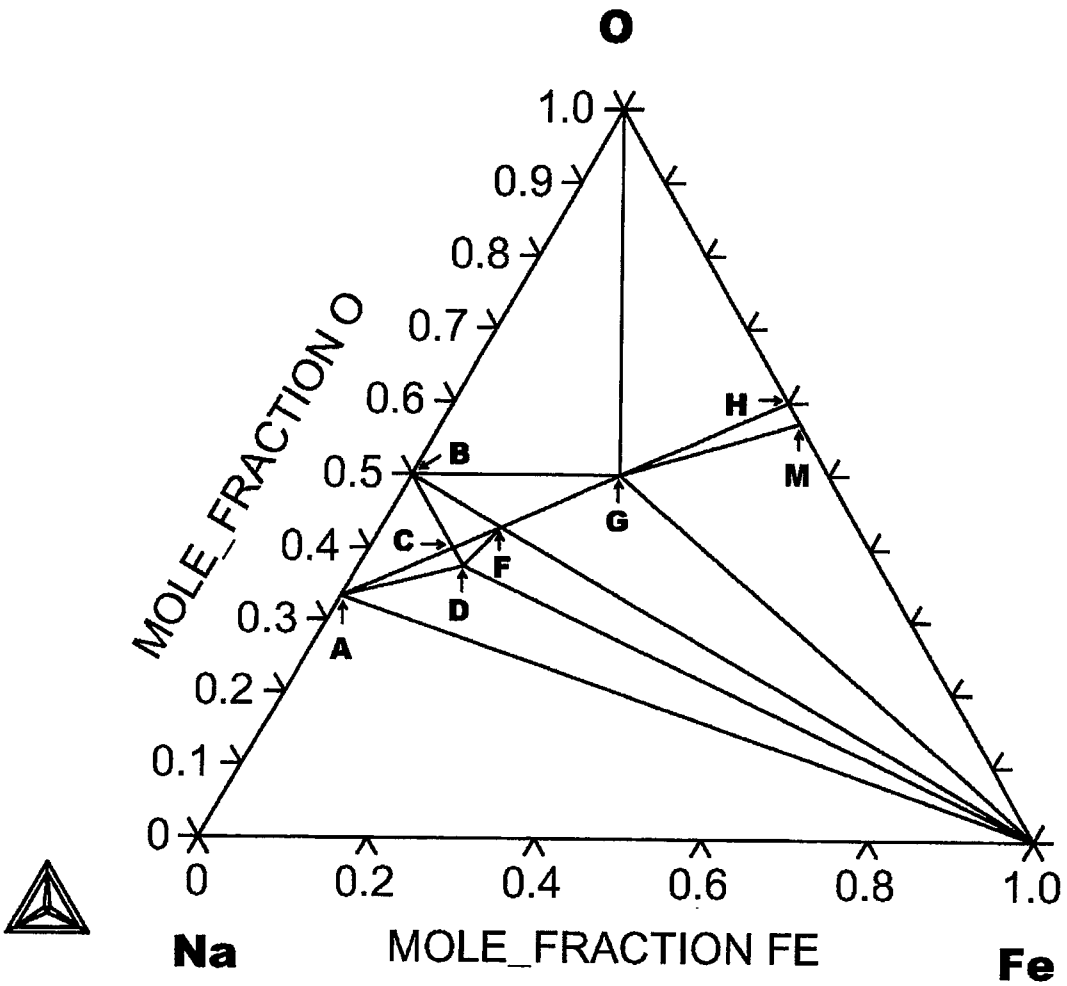

Fig. 14: Isothermal cross sections of the Na-Fe-O in 298-536K.
(A: Na_2O, B: Na_2O_2, C: Na_5FeO_4, D: Na_4FeO_3, F: Na_3FeO_3, G: $NaFeO_2$, H: Hematite, M: Magnetite)

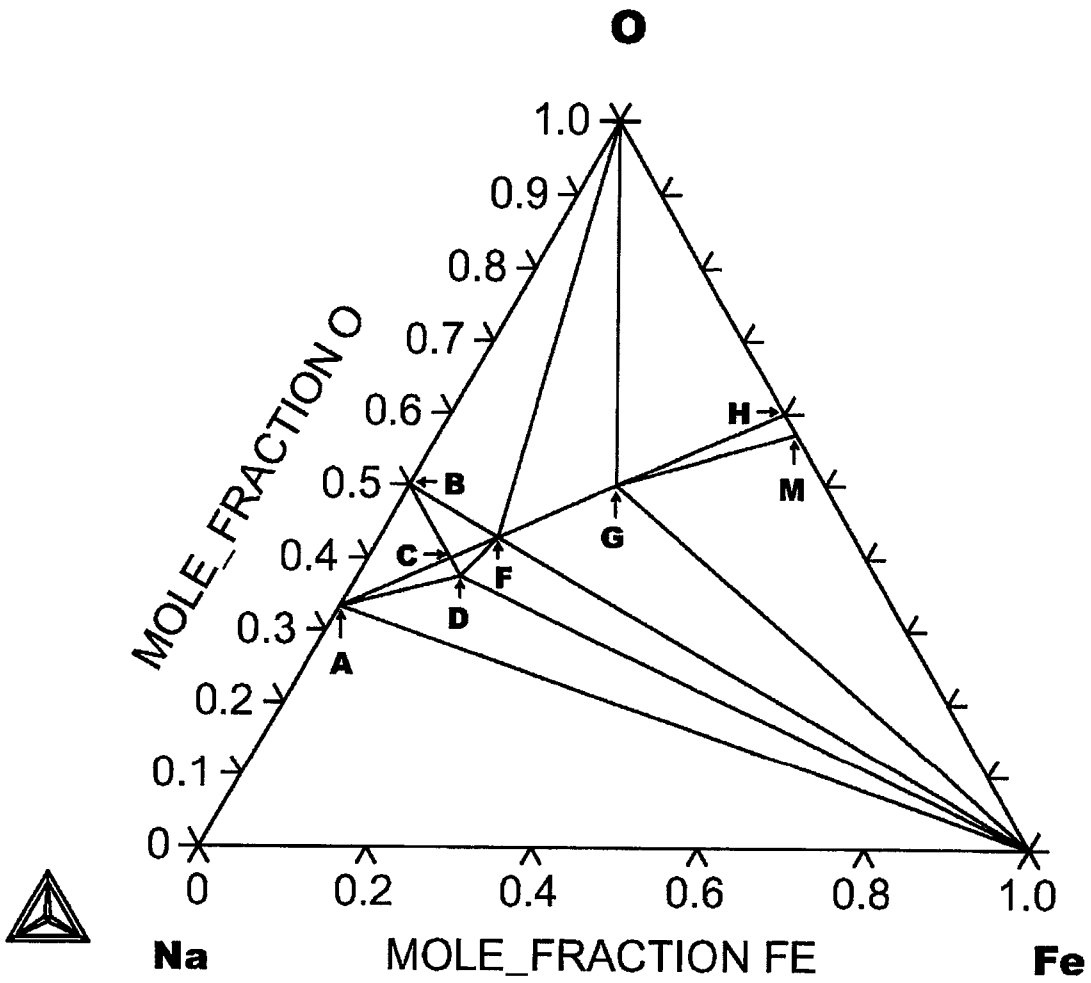

Fig. 15: Isothermal cross sections of the Na-Fe-O in 536-637K.
(A: Na_2O, B: Na_2O_2, C: Na_5FeO_4, D: Na_4FeO_3, F: Na_3FeO_3, G:$NaFeO_2$, H: Hematite, M: Magnetite)

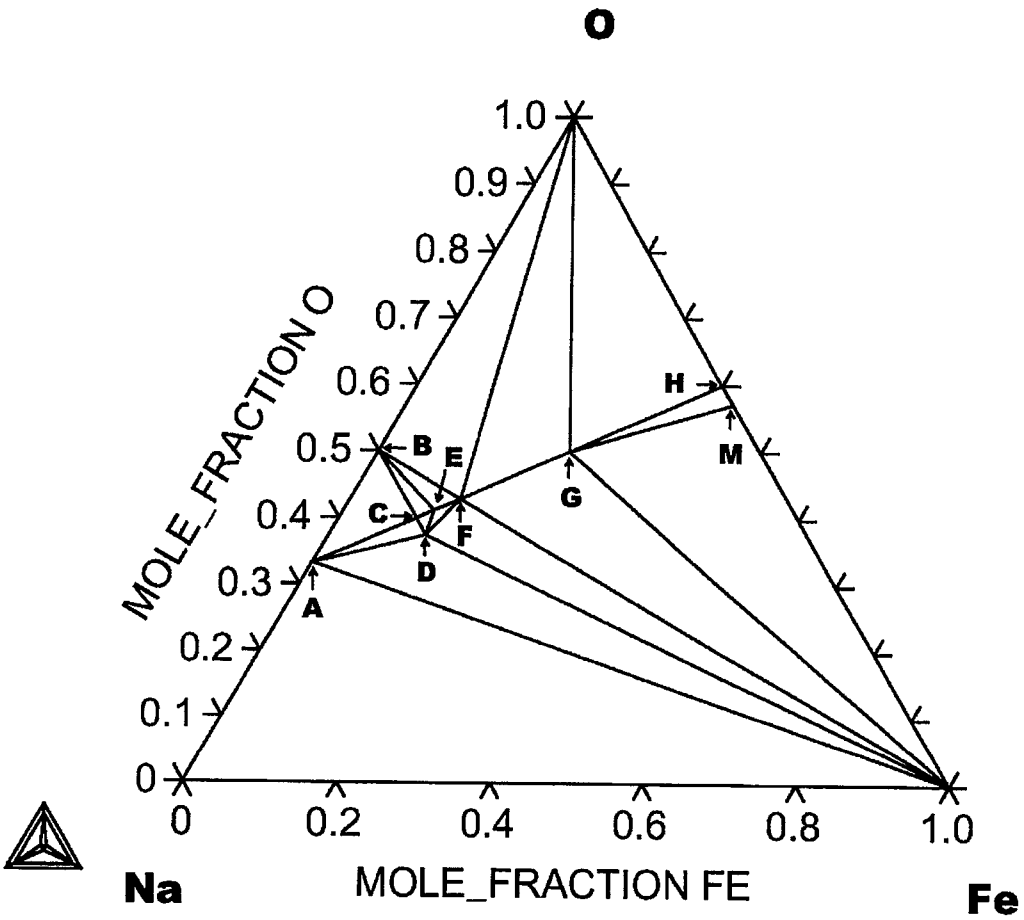

Fig. 16: Isothermal cross sections of the Na-Fe-O in 637-694K

(A: Na_2O, B: Na_2O_2, C: Na_5FeO_4, D: Na_4FeO_3, E: $Na_8Fe_2O_7$ F:Na_3FeO_3, G:$NaFeO_2$, H: Hematite, M: Magnetite)

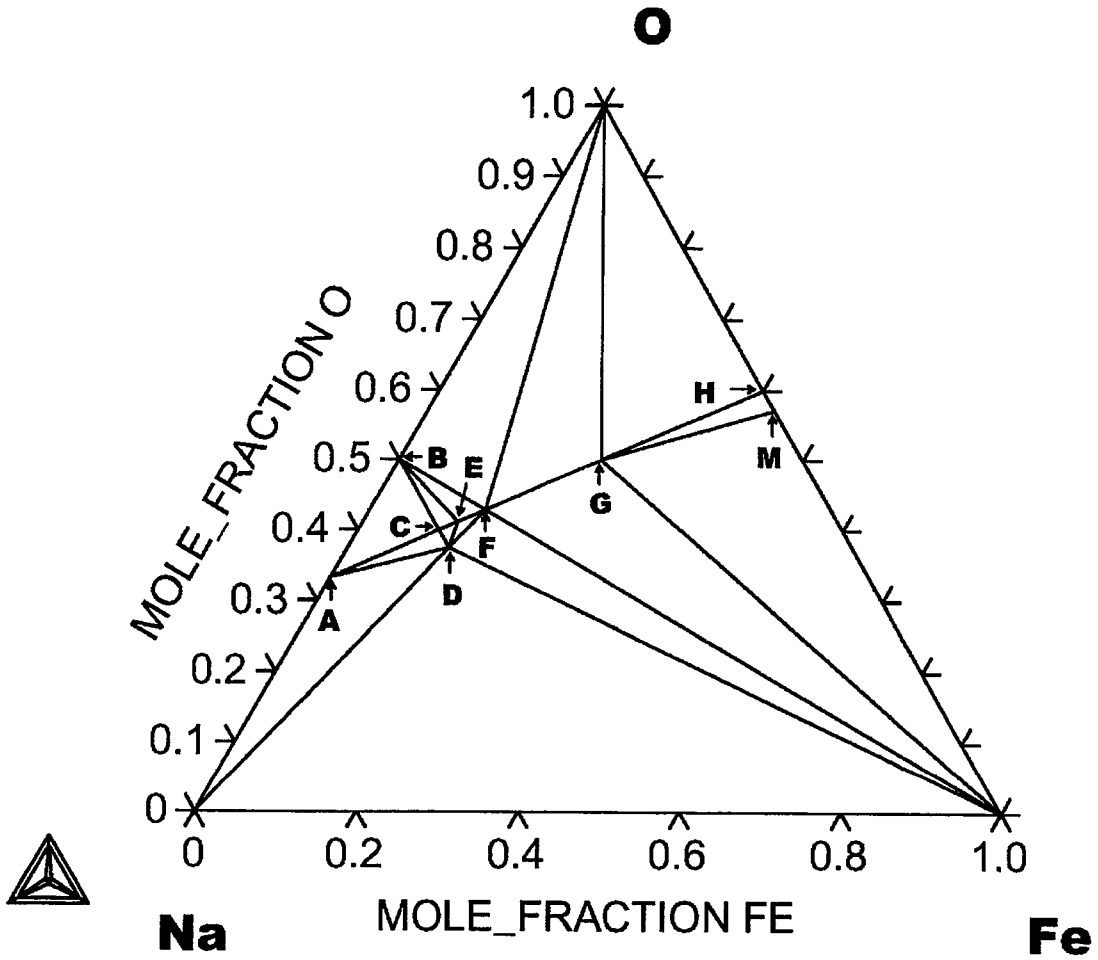

Fig. 17: Isothermal cross sections of the Na-Fe-O in 694-838K
(A: Na_2O, B: Na_2O_2, C: Na_5FeO_4, D: Na_4FeO_3, E: $Na_8Fe_2O_7$ F: Na_3FeO_3, G:$NaFeO_2$, H: Hematite, M: Magnetite)

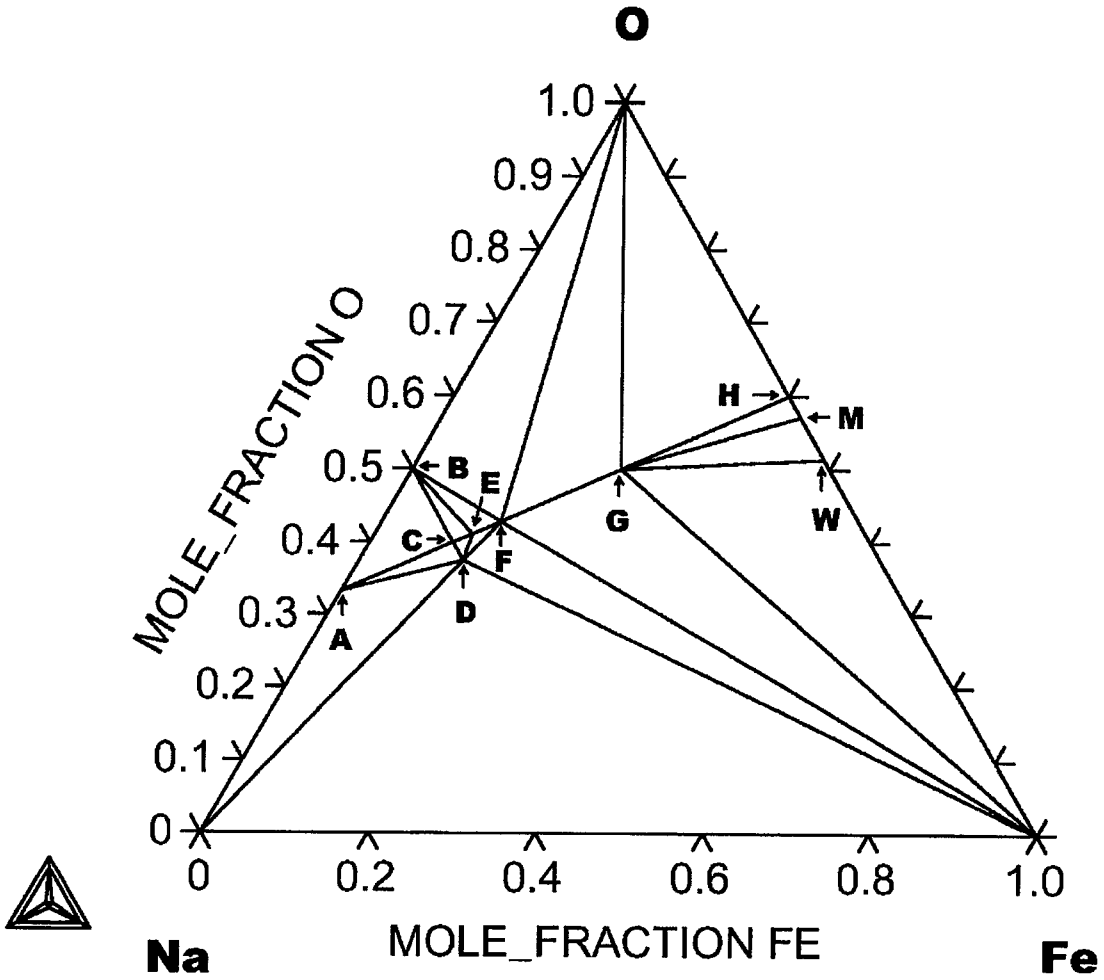

Fig. 18: Isothermal cross sections of the Na-Fe-O in 838-944K
(A: Na_2O, B: Na_2O_2, C: Na_5FeO_4, D: Na_4FeO_3, E: $Na_8Fe_2O_7$ F: Na_3FeO_3, G:$NaFeO_2$, H: Hematite, M: Magnetite, W: Wustite)

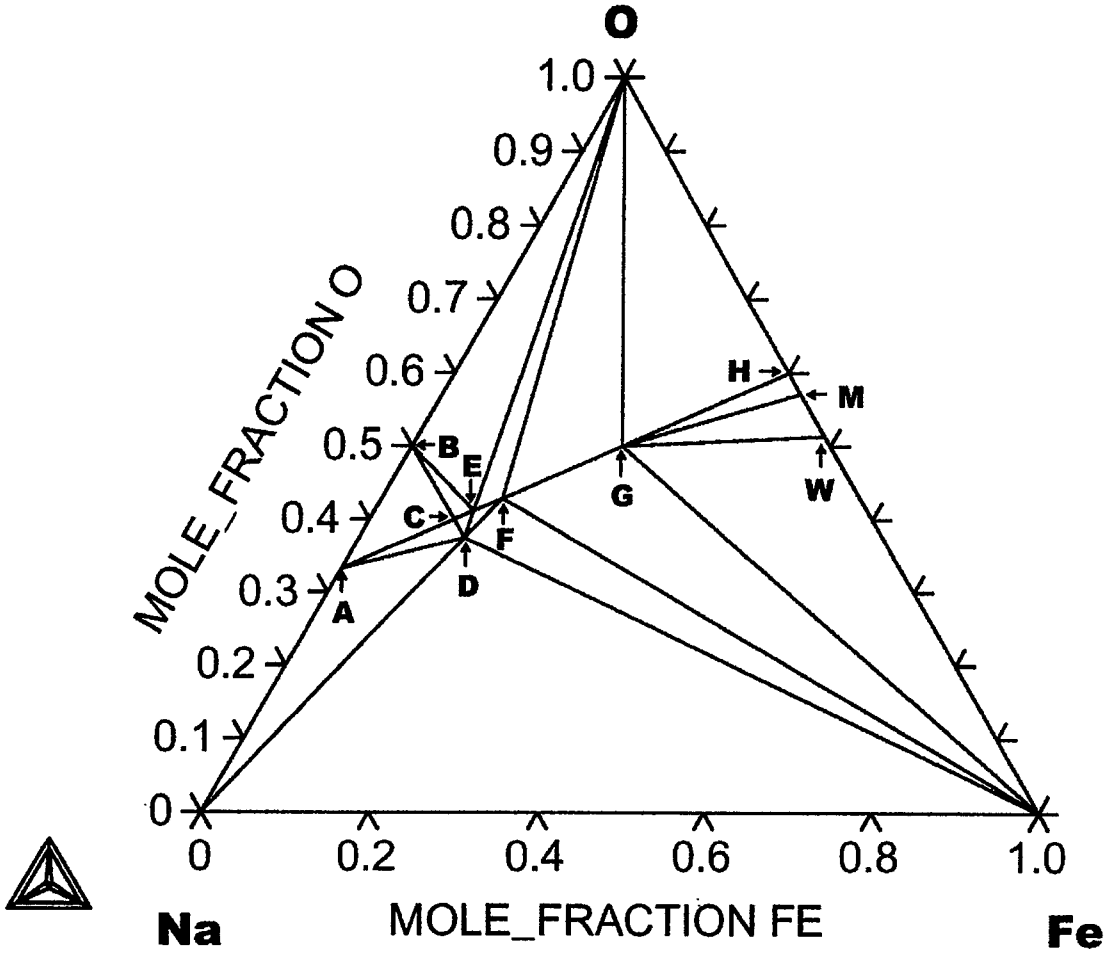

Fig. 19: Isothermal cross sections of the Na-Fe-O in 944-1000K
(A: Na_2O, B: Na_2O_2, C: Na_5FeO_4, D: Na_4FeO_3, E: $Na_8Fe_2O_7$ F:Na_3FeO_3, G:$NaFeO_2$, H: Hematite, M: Magnetite, W: Wustite)

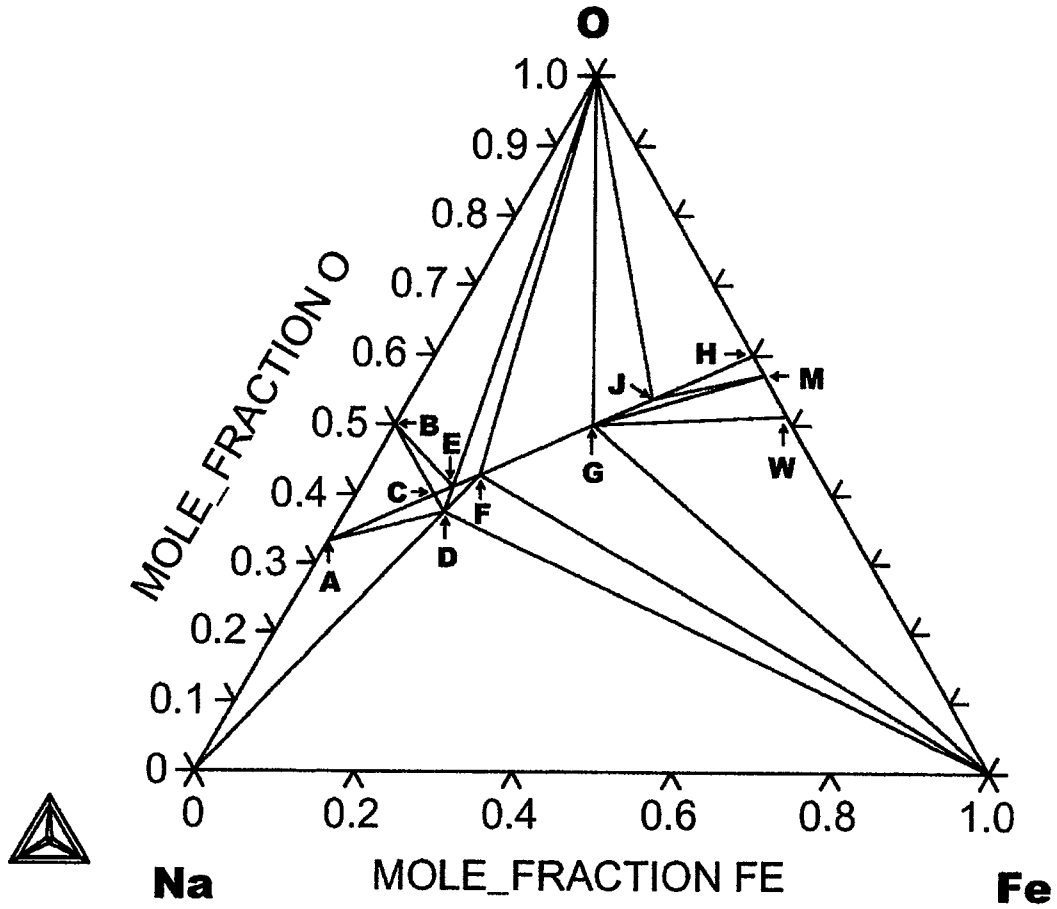

Fig. 20: Isothermal cross sections of the Na-Fe-O in 1030-1200K
(A: Na_2O, B: Na_2O_2, C: Na_5FeO_4, D: Na_4FeO_3, E: $Na_8Fe_2O_7$ F:Na_3FeO_3, G:$NaFeO_2$,
J: $Na_3Fe_5O_9$, H: Hematite, M: Magnetite, W: Wustite)

3.3.2. Chemical potential diagrams

To understand the chemical stability of the Na-Fe oxides, chemical potential diagrams were made as functions of oxygen potential and sodium pressure. So, the stable regions for each phase in the Na-Fe-O system were quantitatively determined. Some typical chemical potential diagrams were shown in Fig. 21-25.

The basic feature of this system is that the main Na-Fe oxides consist of the 4 main Na-Fe oxides, i.e., $NaFeO_2$, Na_3FeO_3, Na_5FeO_4 and Na_4FeO_3.because they are stable in the whole temperature range of the research.

It should be noted that the phase $Na_4FeO_3(s)$ only exists at low oxygen potentials compared to the other Na-Fe complex oxides. The calculated highest oxygen potential at 800K in which $Na_4FeO_3(s)$ can stably exist is as low as about –536 kJ mol^{-1}. On the other hand, stable area for $NaFeO_2(s)$ and $Na_3FeO_3(s)$ can be relatively very wide.

The high temperature phase $Na_8Fe_2O_7$ appears over about 637 K and tends to replace Na_5FeO_4 when temperature goes much higher. The related transition temperatures are a little hard to be determined precisely because of possible errors in estimating the heat capacities of the corresponding complex oxides.

When temperature is over 1030 K, it can also be seen that another high temperature phase $Na_3Fe_5O_9$ becomes stable between $NaFeO_2$ and Na_3FeO_3 though its stable region is relatively very narrow.

According to the equilibrium calculation, $Na_4Fe_6O_{11}$ is not thermodynamically favorable so that it can not be found in these phase diagrams. That is why it is taken as a metastable phase when temperature is lower than about 1270 K as discussed in section 3.1.3.

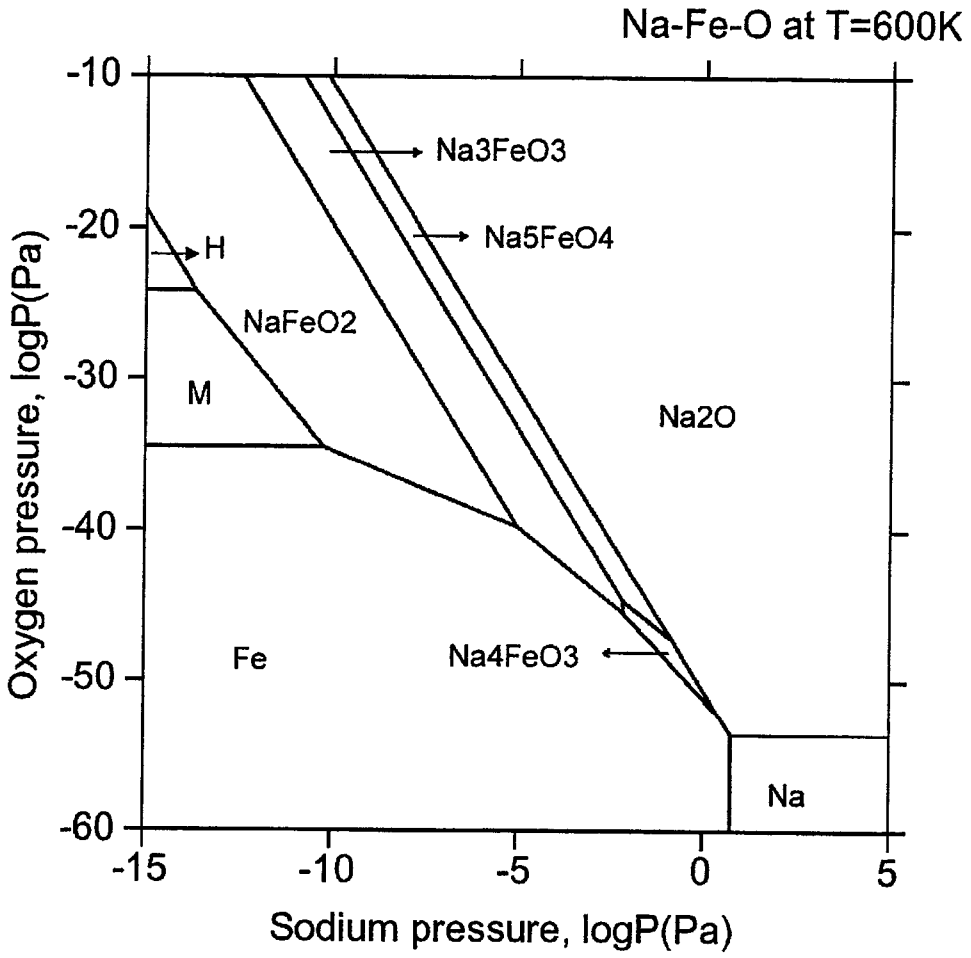

Fig. 21: Predominance diagram of the Na-Fe-O system, T=600K

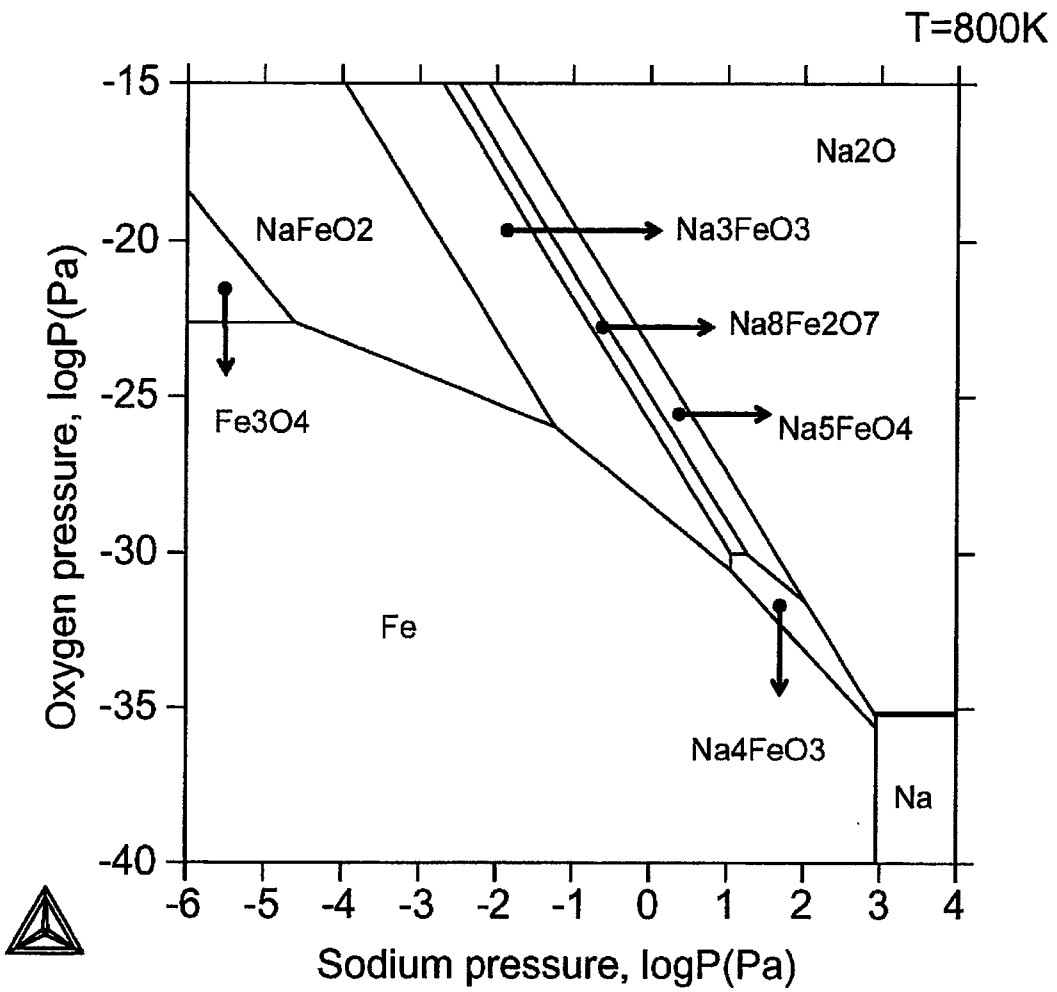

Fig. 22: Predominance diagram of the Na-Fe-O system, T=800K

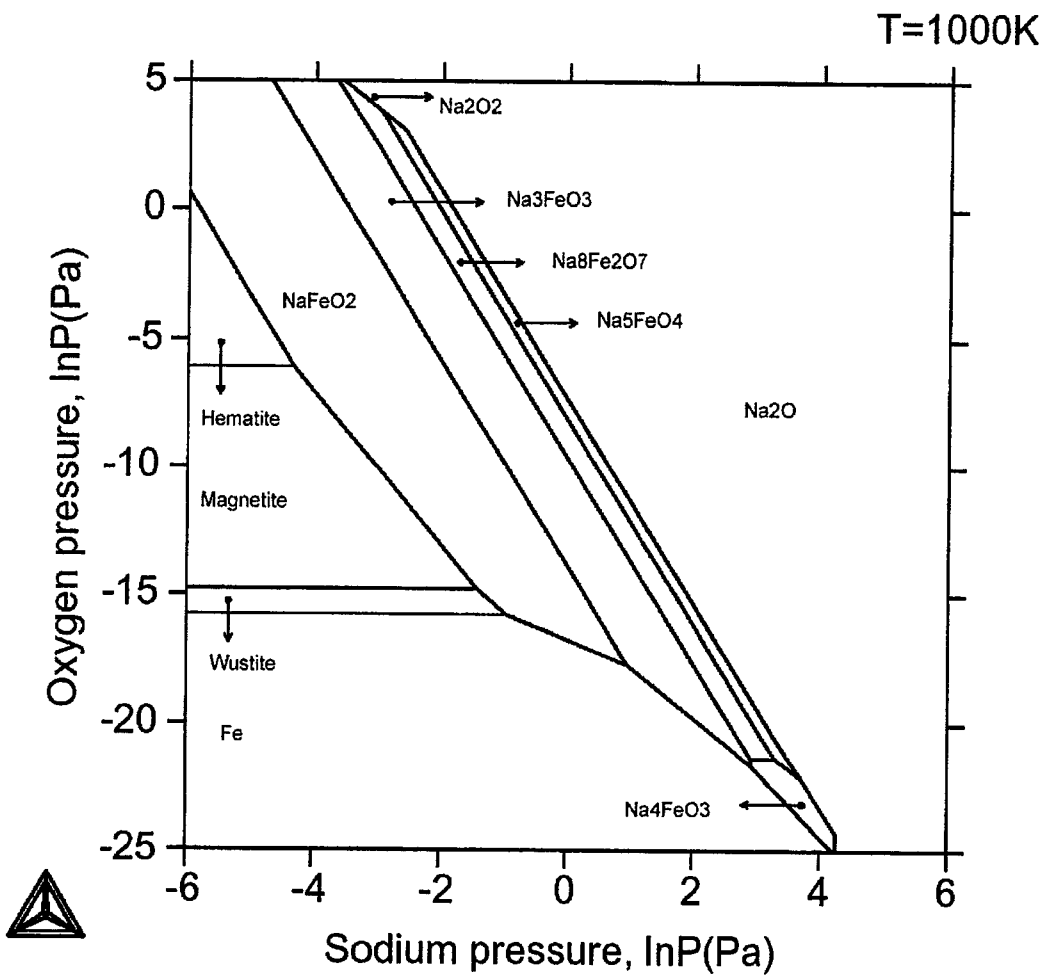

Fig. 23: Predominance diagram of the Na-Fe-O system, T=1000K

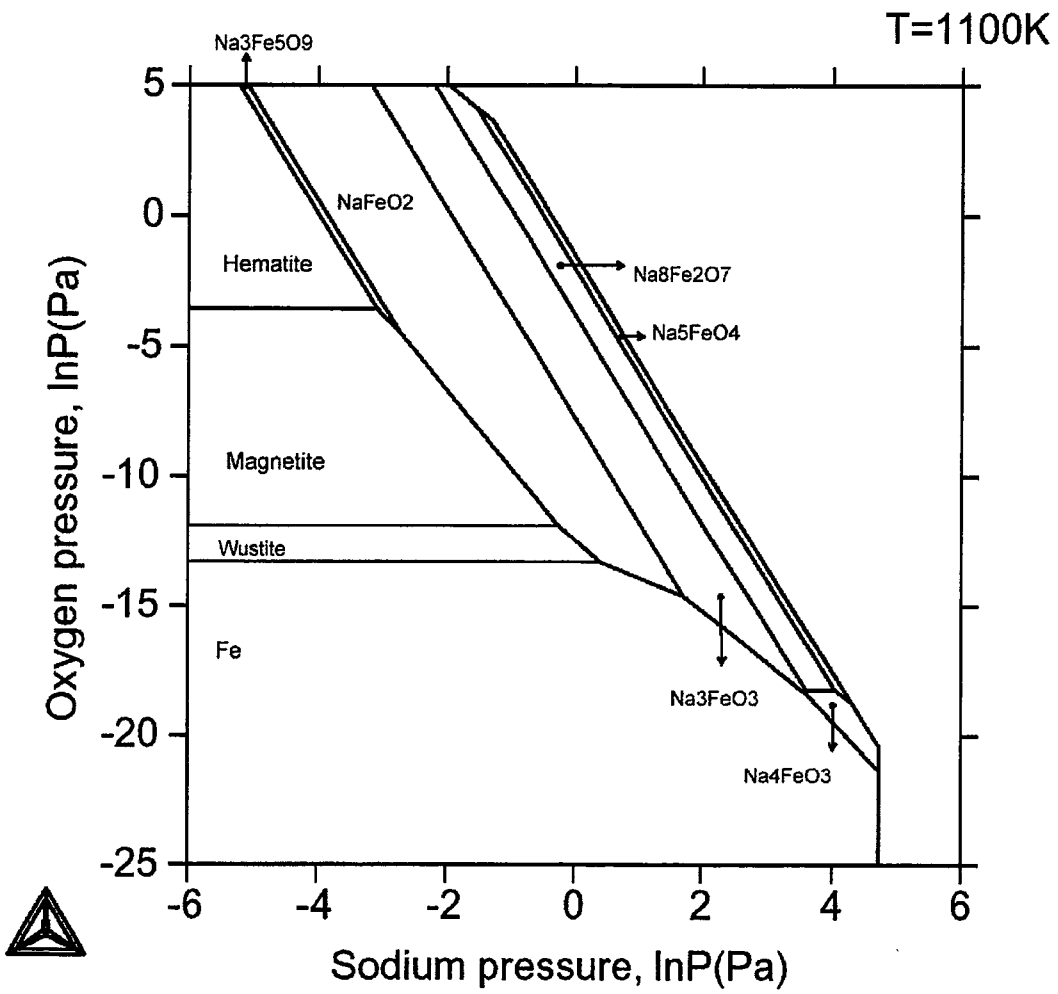

Fig. 24: Predominance diagram of the Na-Fe-O system, T=1100K

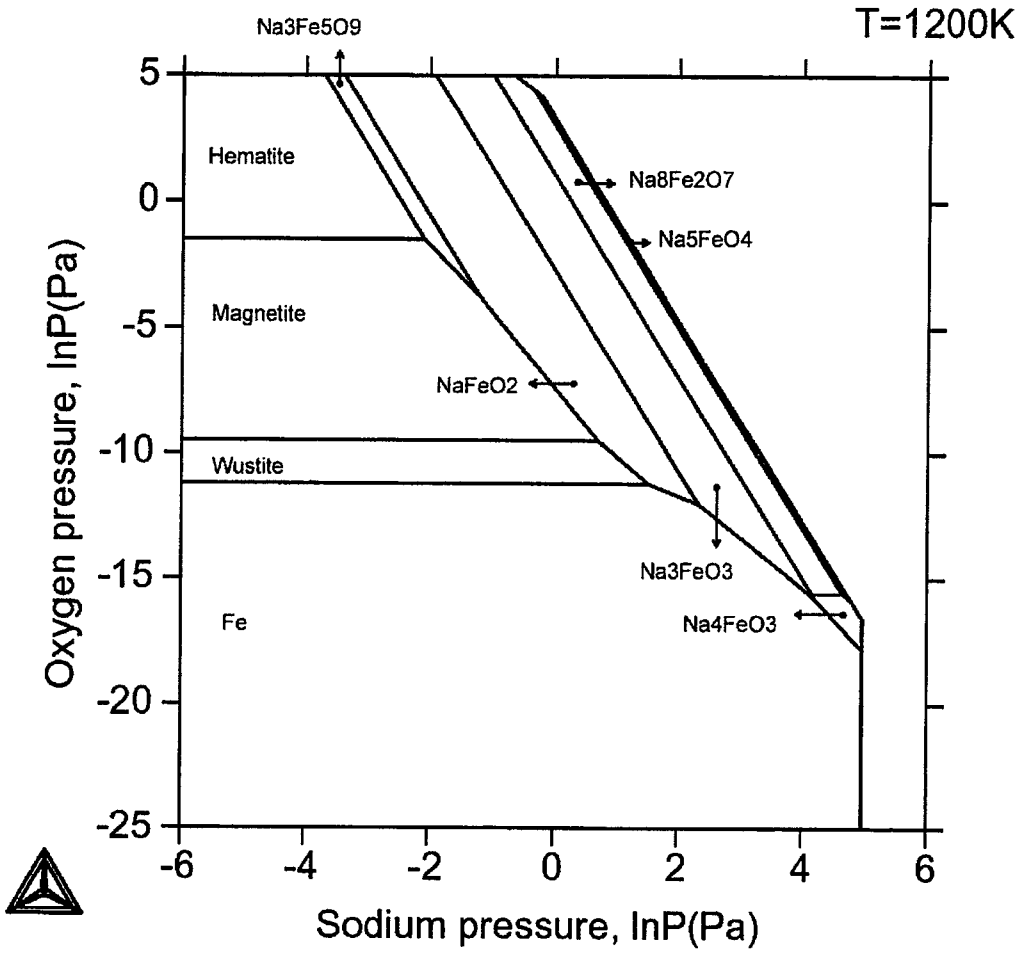

Fig. 25: Predominance diagram of the Na-Fe-O system, T=1200K

3.4 High temperature stability of Na-Fe oxides

To confirm the thermochemical stability of the main Na-Fe oxides, vaporization behaviors of Na-Fe complex oxides, such as $NaFeO_2$, Na_4FeO_3, Na_3FeO_3 and Na_5FeO_4, and the high temperature phases $Na_8Fe_2O_7$, $Na_3Fe_5O_9$ and $Na_4Fe_6O_{11}$, were investigated by means of vapor pressure measurements.

It was found that sodium vapor was released from these compounds at high temperatures. The pressure-temperature relationships were illustrated in Fig. 24. The main reason for that could be explained by that the partial vapor pressure of sodium in the environment is lower than the equilibrium pressure required for the existence of these Na-Fe oxides. The vapor pressure measurements were conducted in vacuum conditions so that all the testing Na-Fe oxides tend to release sodium gas as long as the temperature is high enough.

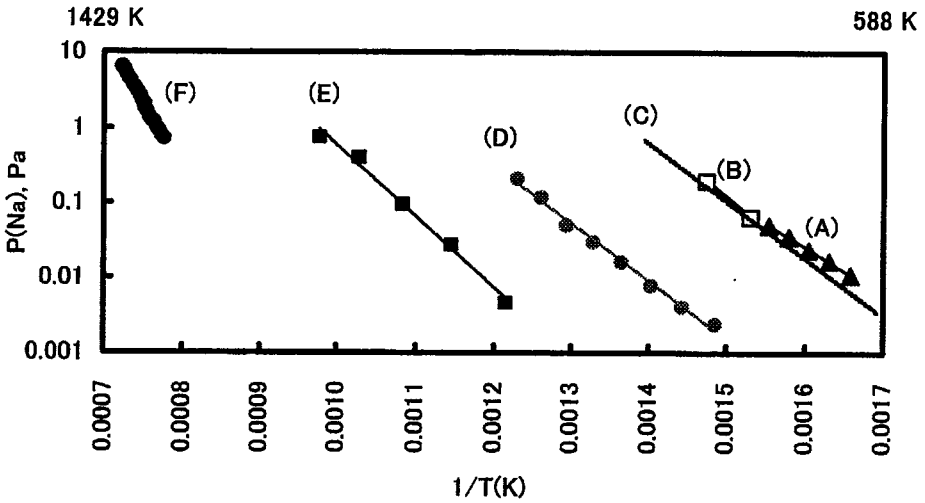

Fig. 26: Vapor pressures over Na-Fe oxides

By X-ray powder diffraction analysis, possible reactions that occurred inside the Knudsen cell were estimated as the following,

(A) $Na_5FeO_4(s) = Na_4FeO_3(s) + Na(g) + 1/2O_2(g)$, (T<640) ·····(28)

(B) $Na_5FeO_4(s) = 1/2Na_8Fe_2O_7(s) + Na(g) + 1/2O_2(g)$, (T>640) ·····(29)

(C) $Na_4FeO_3(s) = Na_3FeO_3(s) + Na(g)$, (550-750K) ·····(30)

(D) $Na_8Fe_2O_7(s) = 2Na_3FeO_3(s) + 2Na(g) + 1/2O_2(g)$, (673-813K) ·····(31)

(E) $Na_3FeO_3(s) = NaFeO_2(s) + 2Na(g) + 1/2O_2(g)$, (823-1023K) ·····(32)

(F) $NaFeO_2(s) = 1/3Fe_3O_4(s) + Na(g) + 1/3O_2(g)$. (1200-1350K) ·····(33)

(G) $Na_3Fe_5O_9(s) = 3NaFeO_2(s) + Fe_2O_3$, (T<1030K). ·····(34)

(H) $Na_4Fe_6O_{11}(s) = NaFeO_2(s) + Na_3Fe_5O_9(s)$, (T<1270K). ·····(35)

Though oxygen potential is too low to be measured for some of the reactions, consistent results can still be found compared to the Na-Fe-O phase diagrams. From the pressure-temperature relationships, Na-Fe-O phase diagram constructed recently was examined and the stability of these Na-Fe oxides at high temperatures was quantitatively determined as functions of temperature, oxygen potential and sodium vapor pressure.

Reaction routes can be concluded as the following,

$Na_5FeO_4 \rightarrow Na_8Fe_2O_7 \rightarrow Na_3FeO_3 \rightarrow NaFeO_2 \rightarrow Fe_3O_4$ ----------(36)

$Na_4FeO_3 \rightarrow Na_3FeO_3$ ----------(37)

$Na_4Fe_6O_{11}(s) \rightarrow Na_3Fe_5O_9(s) + NaFeO_2(s)$ ----------(38)

$Na_3Fe_5O_9(s) \rightarrow NaFeO_2(s)$ ----------(39)

3.4 Reliability evaluation of the results obtained by JNC

Combined the experiments results obtained in JNC and other results reported in the literatures, the thermodynamic database and phase diagrams were constructed. It is significant to check the results by comparing with the experiment results known up to now.

The partial phase diagram in the region of Na(l)-Na_4FeO_3(s)-Na_3FeO_3(s)-Fe(s) over 693K is identical with the schematic diagram drawn by Sridharan et al.[16-17] as shown in Fig. 17-18. It indicates that the present theoretic study agrees well with their experimental results. Outside the above zone, formation of $Na_8Fe_2O_7$(s) over about 637K is thermodynamically favorable according to this calculation. This prediction should be consistent with that of Lindemer's at higher temperatures if Na_2FeO_2(s) were excluded from their study[10].

Due to the importance in nuclear industry, special attention was paid to low oxygen potentials. Na_4FeO_3(s) is considered as one of the main corrosion products in the sodium-leak incident of the MONJU FBR. In this calculation, it is found that Na(l), Fe(s) and Na_4FeO_3(s) coexist over 694K and Na(liq)-Na_2O(s)-Fe(s) is more stable at lower temperatures. The calculated transition temperature is much higher than 629K found by Sridharan [13] but quite close to the 723K reported by Bhat and Borgendete [][14].

It was a pity that the partial pressures of oxygen in the reactions discussed above were too low to be measured by the high temperature mass spectrometer. However, phase identifications, measurements of temperature and partial vapor pressures of sodium

provided some experimental evidence that is consistent with the phase diagrams constructed in the present study. For example, same reaction routes listed in the previous section were often found during the measuring processes of other analysis methods, i.e., TG-DTA, DSC and Raman spectrometry for Na_4FeO_3, Na_3FeO_3 and Na_5FeO_4.

During the phase diagram calculation, it is also found that the phase diagrams are very sensitive to the Gibbs energy of formation of the main ternary Na-Fe oxides. So the assessment of thermodynamic data becomes very important to obtain correct phase diagrams. For example, even a 0.7 kJ mol^{-1} positive shift in $\Delta_f G°(Na_4FeO_3)$ and $\Delta_f G°(Na_3FeO_3)$ may refuse coexistence of the two phases and greatly changed the ternary phase diagram. Usually, an experiment error of a few kJ mol^{-1} seems quite reasonable. It reflects the difficulty of construction of Na-Fe-O phase diagram. This might be the main reason why there exists large discrepancy in the Na-Fe-O phase diagrams published by some pioneers. Fortunately, thermodynamic evaluations of Na_3FeO_3(s) in the present study were directly based on the relationship between Na_4FeO_3(s) and Na_3FeO_3(s) [22,25]. Thus, the user database can be considered as self-consistent so that calculated phase diagrams constructed seem quite consistent with the experiment results for the time being.

Details of the comparison with our experimental results and those reported in literatures are also given in Table 16. For the 7 kinds of Na-Fe complex oxides investigated in JNC, all the experimental results and thermodynamic analysis agree quite well. It seems that the JNC version of Na-Fe-O phase diagram is the most reliable one.

Table 16: Comparison of JNC Na-Fe-O phase diagram with experimental results

Check Points	Conclusion by the JNC Phase diagram	Experiment results	March
Ternary phase diagram	298－1200K (as shown in Fig.14-20)	Partial phase diagram by Sridharan: The same pattern can be found in region of Na-Na_4FeO_3-Na_3FeO_3-$NaFeO_2$-Fe (773-823K)	○
$Na_8Fe_2O_7$	$Na_8Fe_2O_7$ is stable only when T>640K.	(1)$Na_3FeO_3+Na_5FeO_4 \rightarrow Na_8Fe_2O_7$ (T>673K) (2) By high temp. mass spectrometer, $Na_5FeO_4 \rightarrow Na_8Fe_2O_7 \rightarrow Na_3FeO_3$	○
Na_4FeO_3	Critical temperature of Na-Na_4FeO_3-Fe T=693K; (2) Coexistence of Na_4FeO_3+Na_3FeO_3	(1) Ref: the critical temperature Bhat[14]: 723K Sridharan[13]: 629K Gross[39]: 760K Lindemer[10]: 650K (2) By high temp. mass spectrometer, 550-750K, $Na_4FeO_3=Na_3FeO_3+Na$	○
Na_3FeO_3	Coexistence of $NaFeO_2$+Na_3FeO_3	By high temp. mass spectrometer, 773-1023K, $Na_3FeO_3 \rightarrow NaFeO_2$	○
Na_5FeO_4	Coexistence of Na_5FeO_4+$Na_8Fe_2O_7$	By high temp. mass spectrometer, 640-690K, $Na_5FeO_4 \rightarrow Na_8Fe_2O_7$	○
$NaFeO_2$	Coexistence of $NaFeO_2$+ Fe_3O_4	By high temp. mass spectrometer, 1200-1350K, $NaFeO_2 \rightarrow Fe_3O_4$	○
$Na_3Fe_5O_9$	$Na_3Fe_5O_9$ is stable only when T>1030K.	Kale et al.[41] They found it decompose when T<1029K. $Na_3Fe_5O_9=3NaFeO_2+Fe_2O_3$	○
$Na_4Fe_6O_{11}$	$Na_4Fe_6O_{11}$ is unstable when T>1030K.	It decomposed at high temperatures. $Na_4Fe_6O_{11}=NaFeO_2+ Na_3Fe_5O_9$	○

4. Thermodynamics of the Na-Fe-O-H-C system

It is known that the volume percentages of H_2O and CO_2 in the atmosphere at room temperature are usually 1.57% and 0.03% respectively. So, their influence on the behaviors of Na-Fe-oxides should be taken into account. Equilibrium calculations in Na-Fe-O-H-C were conducted by using the user database described before. Experimental confirmation was also made by means of the gas-inlet KEMS and other experiment.

4.1 Equilibrium calculations of the Na-Fe-O-H-C system

MALT2 code was employed to analyze the multi-component system. To simplify the problem, the simulations were made considering the following aspects.

- System:
  Na-Fe-O-H and Na-Fe-O-C were considered to simplify the problem, then Na-Fe-O-H-C system was calculated
- Temperature:
  The low operation temperature of the sodium coolant in FBR is usually around 573 K while the high output temperature is around 800K. So, the simulation was made at 573 K and 800 K.
- Environmental conditions:
  Estimation of the vapor pressures of H_2O and CO_2 at high temperatures in the environment is needed for the further discussion. The gas composition in the atmosphere at room temperature is listed in Table 17. When the temperature increases, the water vapor pressure in air will increase too. The water needed for this increase may come from the water stored in the surrounding substances, like wall, floor, etc... It is well known that the pressure of the saturated water vapor is 1 atmosphere at 100°C. In an open space, however, the water vapor pressure actually can not go over 1 atmosphere even at higher temperatures like 800 K. In some local reaction zone that is isolated by the reactants and products from the atmosphere, the water vapor pressure may decrease to very low level. So, the range of water vapor pressure in the present simulation will be done from vacuum to 101325 Pa. As for carbon dioxide, the variation of its content in the air with increase of temperature is hard to be estimated. Unlike water vapor, CO_2 may have little possibility to increase unless there exists some carbon source in the environment, for example, the burning of wooden goods. In contrast, its pressure would decrease if it were consumed by reacting with other substances in the system at high temperatures. Thus, $P_{CO2}<33$Pa was paid more attention in the present simulation.

Table 17: Gas composition in the atmosphere at room temperature

Gas	Volume %	Partial pressure, Pa
N_2	78.08	79114
O_2	20.95	21228
H_2O	1.57	1600
Ar	0.93	942
CO_2	0.033	33

Simulation of Na-Fe-O-H at 573 K was made first so that the influence of water vapor on Na-Fe oxides could be understood without considering CO_2. Assuming the water vapor pressure in environment is fixed, the chemical potential diagram can be constructed by MALT2 easily. The calculations show that NaOH is thermodynamically favorable together with $NaFeO_2$ even if water vapor pressure is very low. An example is given in Fig. 27. It shows that other Na-Fe complex oxides such as Na_5FeO_4, $Na_8Fe_2O_7$ as well as Na_3FeO_3 disappear when water vapor pressure is fixed at 1 Pascal at 573 K.

The following reaction routes would be possible,

$H_2O+Na_5FeO_4 \rightarrow 2NaOH+Na_3FeO_3$ ----------(40)

$H_2O+Na_3FeO_3 \rightarrow 2NaOH+NaFeO_2$ ----------(41)

and so on

Similar calculation in Na-Fe-O-C system has been done at 573 K too. The equilibrium calculation indicates that CO_2 has much higher influence on Na-Fe oxides. Even if the pressure of carbon dioxide is extremely low, Na_2CO_3 would be the most stable phase in the system. An example was given in Fig. 28, in which the pressure of CO_2 was fixed at 1E-6 Pa. According to the equilibrium calculations, the main stable compounds in the system would be $NaFeO_2$ and Na_2CO_3 if $P_{CO2}=10^{-6}$ Pa. Other Na-Fe oxides tend to be no longer stable because of the presence of CO_2. CO_2 may react with Na-Fe oxides and Na_2CO_3 may be formed. Possible reactions would be like,

$CO_2+Na_5FeO_4 \rightarrow Na_2CO_3+ Na_3FeO_3$ ----------(42)

$CO_2 + Na_3FeO_3 \rightarrow Na_2CO_3 + NaFeO_2$ ----------(43)

and so on.

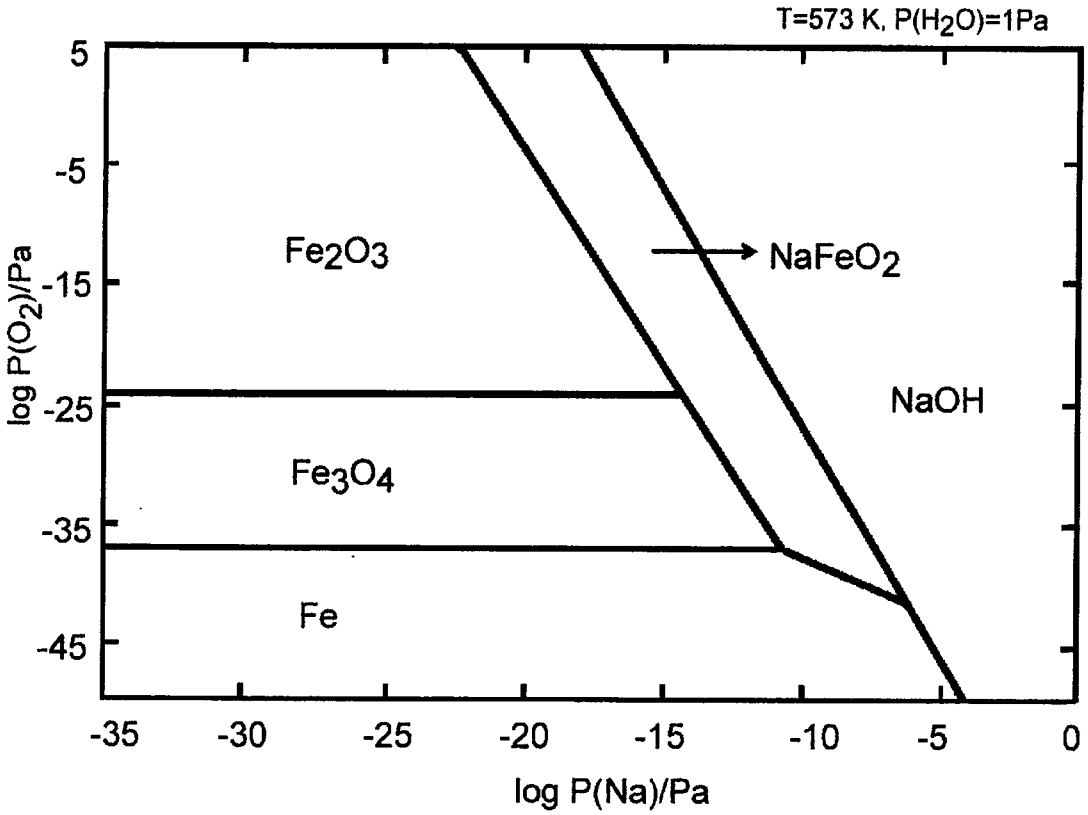

Fig. 27: Na-Fe-O-H system, T=573K, $P(H_2O)$=1Pa

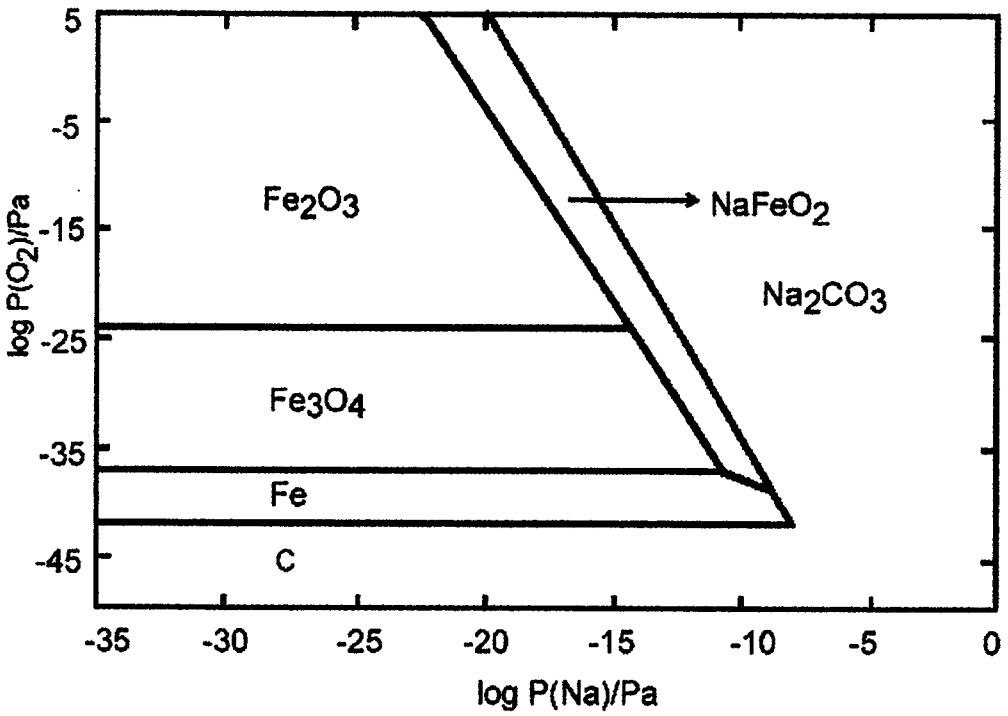

Fig. 28: Na-Fe-O-C system, T=573 K, $P(CO_2)$=1E-6 Pa

Since the high output temperature of coolant sodium in FBRs is usually about 773-823 K, simulation calculations were also made at 800 K. To show the effects of water vapor pressure on the equilibrium states in the Na-Fe-O-H system, the calculation results were illustrated in Fig. 29 as a function of water vapor pressure. It can be seen that water vapor has great influence on the behaviors of Na-Fe oxides. When P_{H2O} <10^{-2} Pa, the chemical potential diagram is almost the same as Fig. 22 in the Na-Fe-O system. It agrees well with the fact that Na_4FeO_3 was found as the corrosion products in an isolated reaction zone where the oxygen potential and water vapor pressure were very low due to the sealing effect of massive sodium. In the normal atmosphere condition, i.e., P_{H2O}>1600 Pa, Na_5FeO_4, $Na_8Fe_2O_7$, Na_3FeO_3 and Na_4FeO_3 should be no longer stable except for $NaFeO_2$. $NaFeO_2$+NaOH are always stable even if the water vapor pressure is as high as 1 atm.

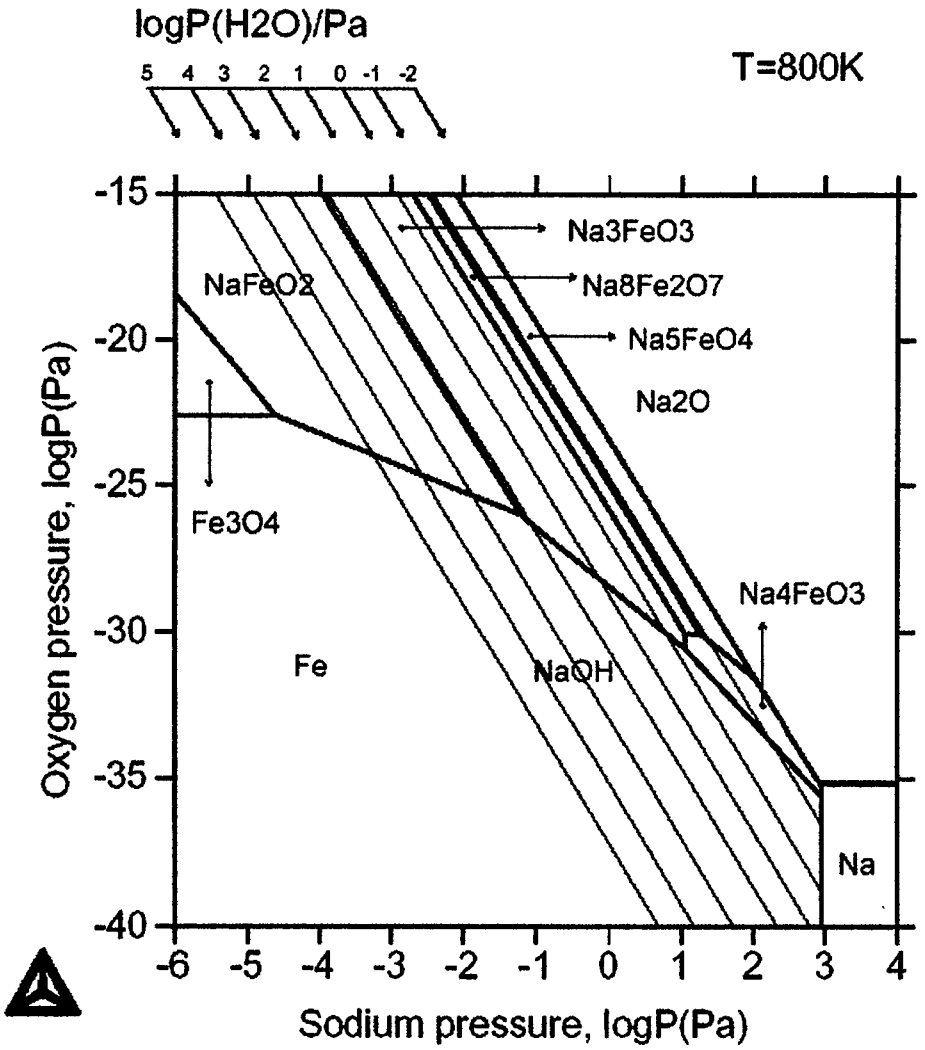

Fig. 29:Na-Fe-O-H system, T=800 K

Simulation calculations of the Na-Fe-O-C system at 800 K were made. It is found that CO_2 also plays very important role to determine the behaviors of Na-Fe compounds. As shown in Fig. 30, when P_{CO2} is higher than about 10^{-4} Pa, the stable pattern would be Na_2CO_3+$NaFeO_2$. If P_{CO2} exceeds about 100 Pa, the Magnetite or Hematite probably would be the most stable iron oxides together with Na_2CO_3, while all Na-Fe complex oxides like $NaFeO_2$, Na_3FeO_3, $Na_8Fe_2O_7$ and Na_5FeO_4 would be no longer stable any more.

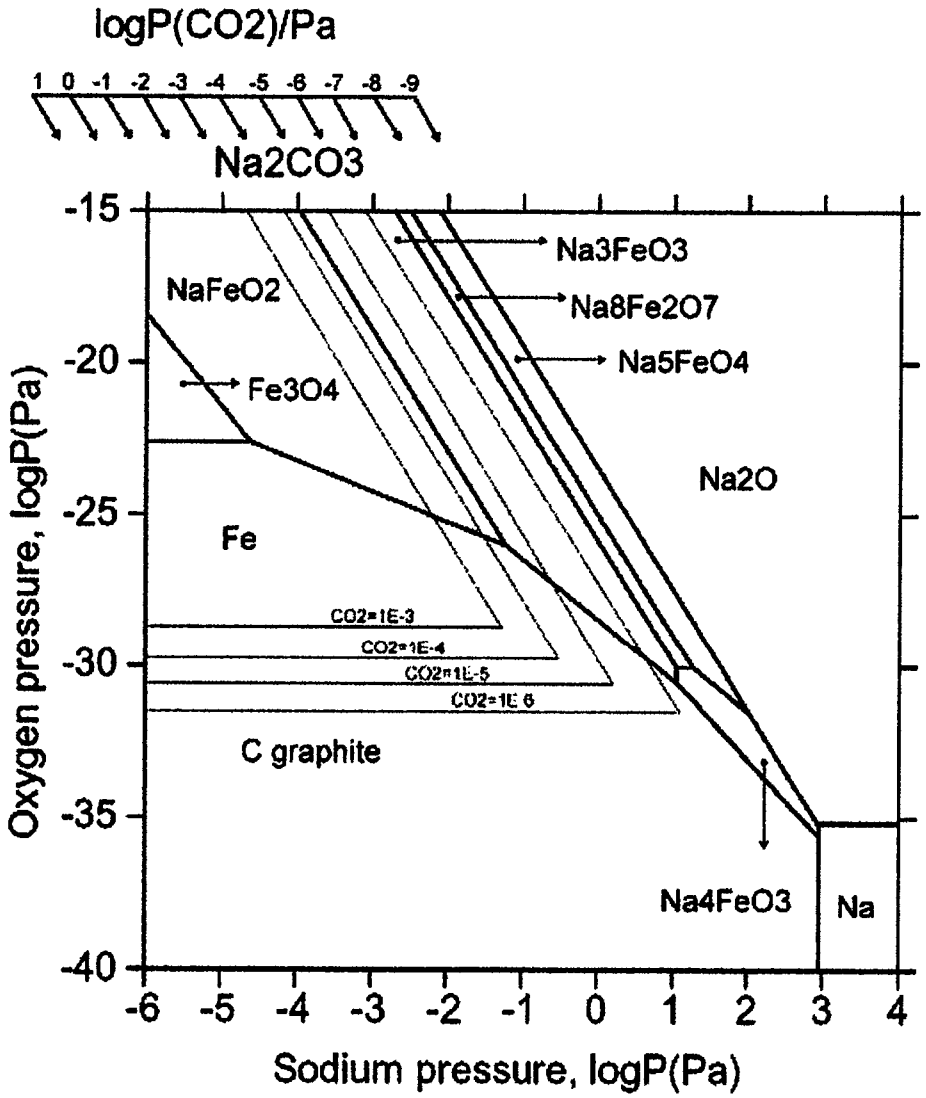

Fig. 30:Na-Fe-O-C system, T=800 K

Keep the above results in mind, equilibrium calculation of sodium ferrates in water vapor and carbon dioxide environments can be treated together by fixing P_{H2O} and P_{CO2} in proper values. The competence of H_2O and CO_2 was investigated by simulation calculation at 800 K.

If the CO_2 pressure in the atmosphere at 800 K is about 33 Pa (similar with that in room temperature), the results show that the phase diagram pattern does not change no matter how large the water vapor pressure is. The chemical potential diagram in this case was shown in Fig. 31.

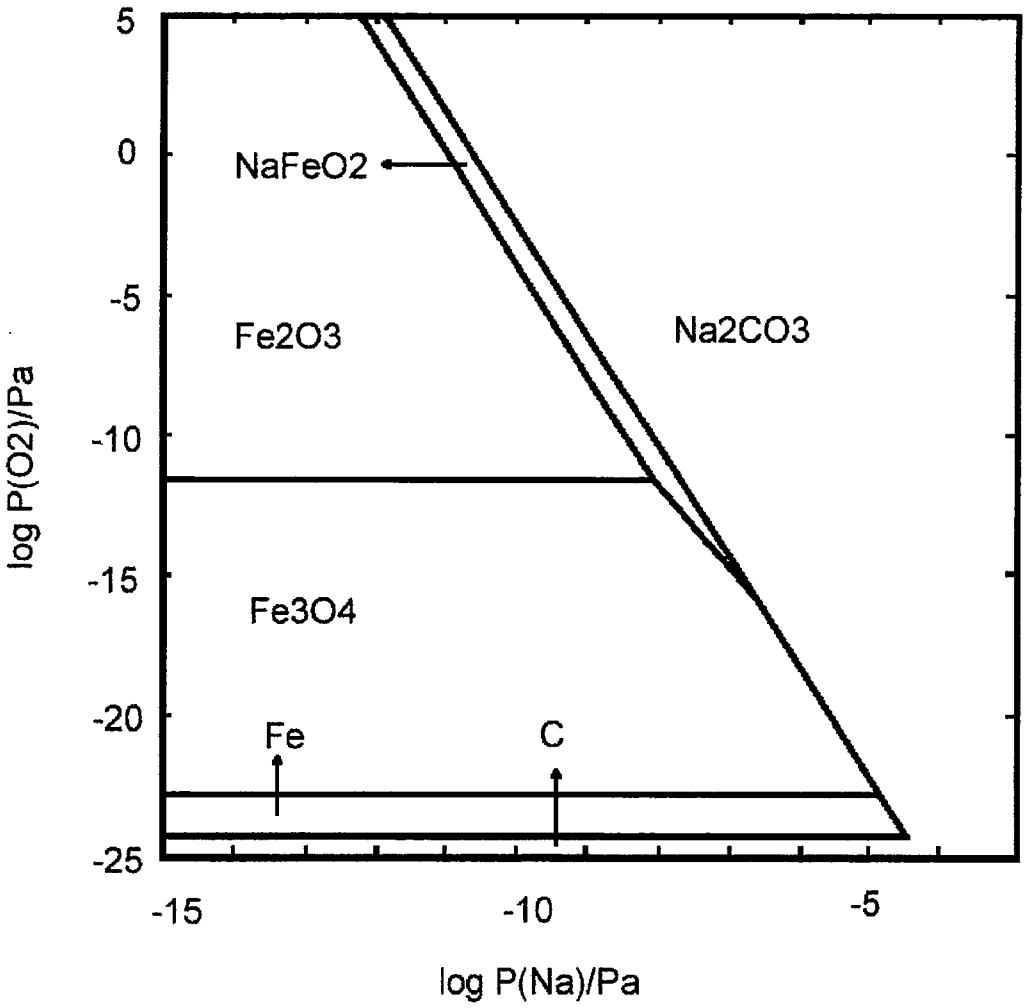

Fig. 31:Na-Fe-O-H-C system, T=800K, $P(CO_2)$=33 Pa, $P(H_2O) \leqq 101325$ Pa

On the other hand, if the water vapor pressure at 800 K is fixed at 1600 Pa, equilibrium calculations can be done as a function of P_{CO2}. Two typical chemical potential diagrams were found in the simulation. One is given in Fig. 32, in which Na_2CO_3 is stable as long as P_{CO2} is in the range from 10^{-4} Pa to 33Pa. When P_{CO2} is lower than about 10^{-4} Pa at 800 K, NaOH will replace Na_2CO_3 to be the stable phase as shown in Fig. 33.

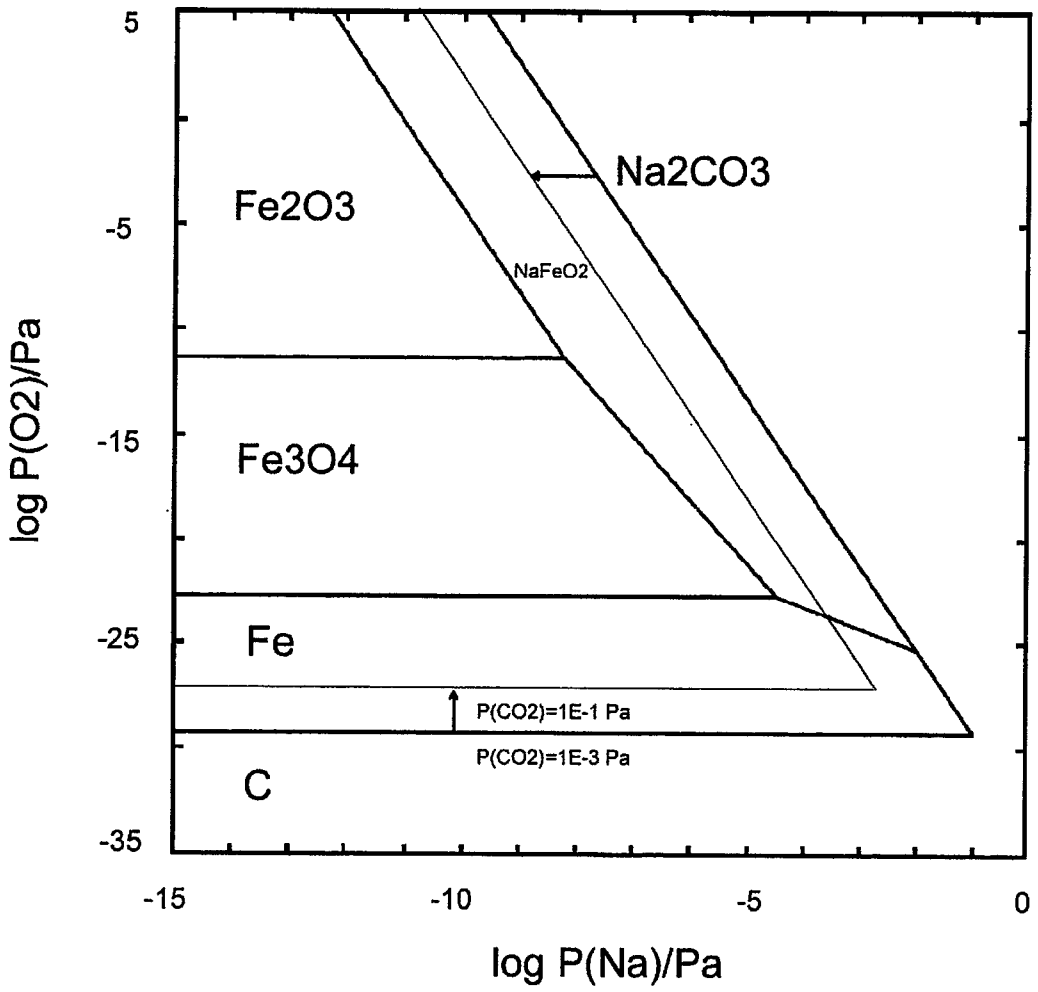

Fig. 32:Na-Fe-O-H-C system, T=800K, $P(H_2O)$=1600 Pa, $P(CO_2)\geqq$1E-3 Pa,

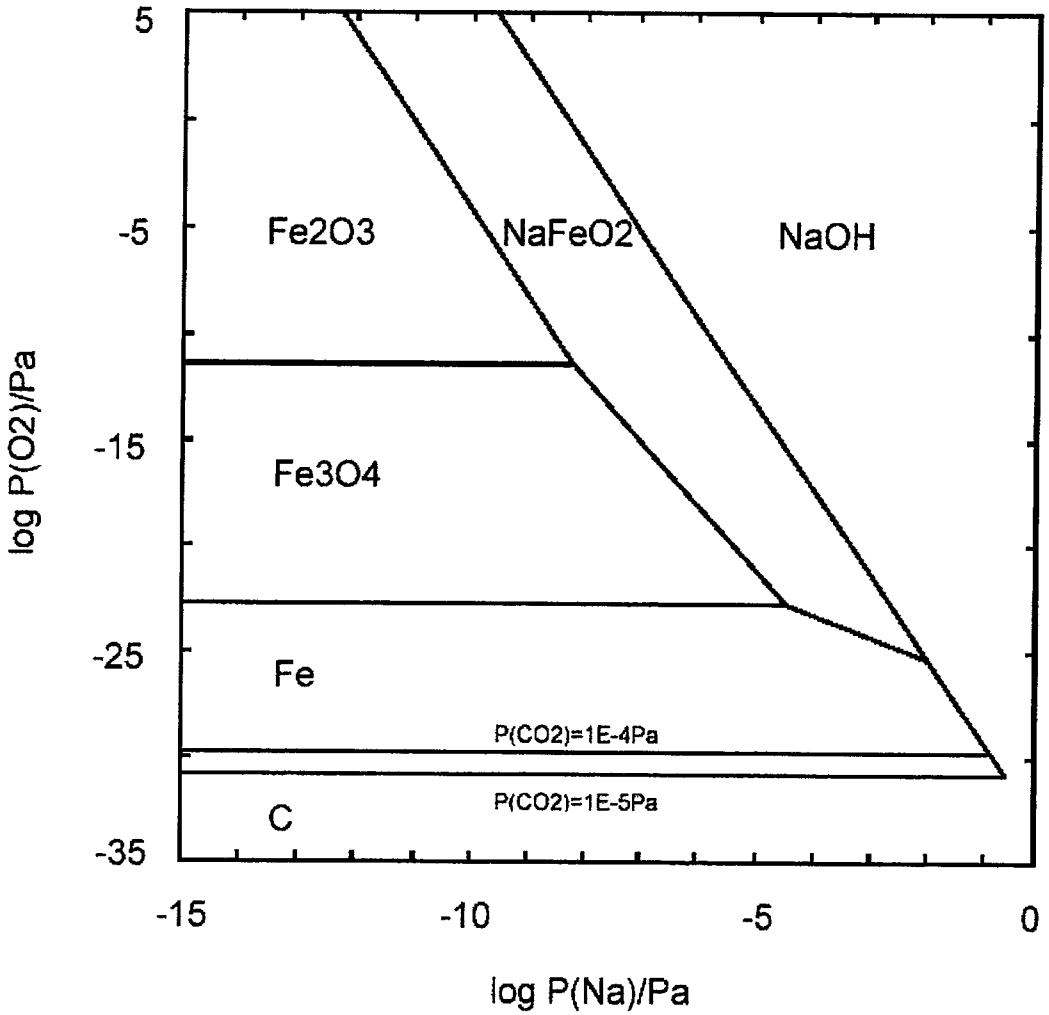

Fig. 33:Na-Fe-O-H-C system, T=800K, $P(H_2O)$=1600 Pa, $P(CO_2) \leqq$1E-4 Pa

From the simulation calculations carried out above, the following conclusions could be made.

- The equilibrium states in Na-Fe-O-H-C is greatly depends on the environmental conditions. Apart from temperature, oxygen potential and sodium pressure, the water vapor pressure and carbon dioxide pressure also have strong influence on behaviors of Na-Fe oxides in the Na-Fe-O-H-C system.
- Molten salts NaOH or Na_2CO_3 has high possibility to be formed in a wide range of temperature and gases conditions which play great role in the so-called "Molten Salt Corrosion Mechanism" of sodium-leak incident of FBRs.
- It seems that the influence from CO_2 surpasses that of H_2O to dominate the chemical potential diagram, i.e., CO_2 may have stronger influence on equilibrium states in Na-Fe-O-H-C system than H_2O does.

4.2 Experiments

4.2.1 Experiment by gas-inlet KEMS

From the above theoretic calculation, water vapor and carbon dioxide have strong effects on Na-Fe oxides. It seems that carbon dioxide shows much higher influence on the stability of Na-Fe oxide than water vapor. The gas-inlet KEMS was employed to investigate Na-Fe oxides behaviors in three kinds of environmental conditions, i.e., H_2O, CO_2 and H_2O+CO_2 by introducing H_2+O_2, CO_2 and H_2+CO_2, respectively. Na_5FeO_4 and Na_3FeO_3 prepared in our laboratory were used as the starting sodium ferrite because it should reflects the influence of water vapor and carbon dioxide shown in phase diagram Fig. 27-31. The experimental results were given in Table 18.

The experiments at high temperature (873-923K) showed that Na_2CO_3 were only slightly formed in the surface of the sodium ferrite even if CO_2 pressure was as high as 1 Pascal level. After about 20-hours testing in H_2O+CO_2 environment, the main phases were Na_5FeO_4, $Na_8Fe_2O_7$ and NaOH together with a small amount of Na_2CO_3. It indicted that Na_5FeO_4 decomposed to $Na_8Fe_2O_7$ in the experimental condition If CO_2 was introduced without H_2O, the product was only $Na_8Fe_2O_7$. It was noticed that thermal decomposition of Na_5FeO_4 might be the dominant process at high temperatures; so, similar tests were also made at lower temperatures. For example, at 523-573K, the partial vapor pressure of sodium could not be detected by the KEMS. It means that the thermal decomposition of Na-Fe oxides was very limited and can be neglected. Then, the influence of water vapor or carbon dioxide could be investigated better. At the initial stage (reaction time of 10 hours), however, apart from the reactant Na_5FeO_4, only NaOH was found in the products by XRD. When the reaction time was increased to about 53 hours, peak of NaOH was increased but no evidence of $NaFeO_2$ was observed as shown in Fig. 34. After about 103 hours, Na_5FeO_4 was almost disappeared while Na_3FeO_3 and $NaFeO_2$ were formed as shown in Fig. 35. It seems that the reducing reaction by water vapor occurred in steps as the following,

$$Na_5FeO_4+H_2O \rightarrow Na_3FeO_3+2NaOH;$$
$$Na_3FeO_3+H_2O \rightarrow NaFeO_2+2NaOH$$

In the CO_2 inlet experiment at 550K for about 100 hours, no evidence of formation of Na_2CO_3 was found either.

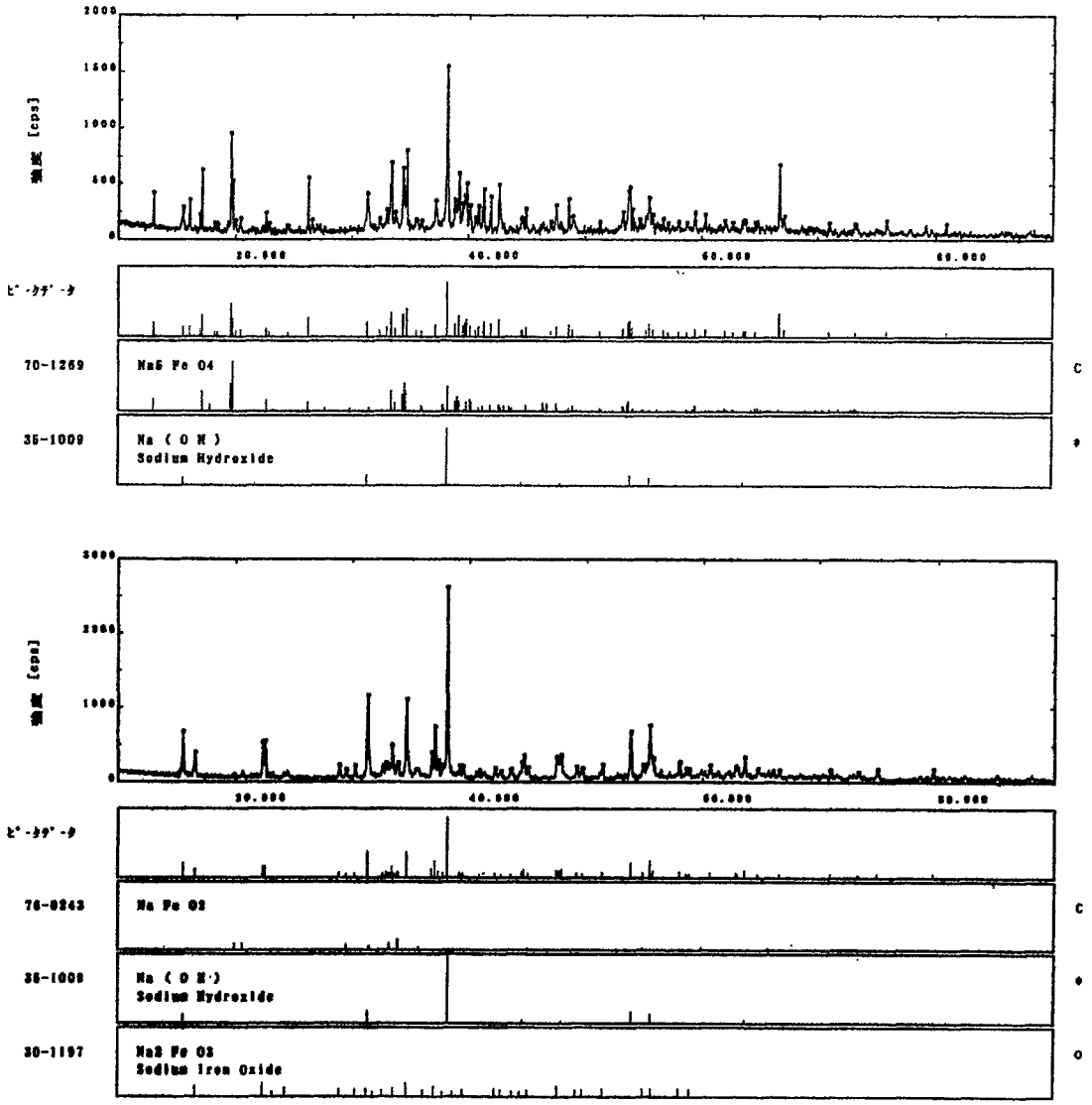

Fig. 34: XRD patterns after Na_5FeO_4 was heated at 573 Kin H_2O environment. (upper:53hurs; lower:106 hours)

All the experimental results listed in Table 18 seem to be against the equilibrium calculations made in the previous sections. Thus, it is necessary to analysis possible reasons for this discrepancy. One possible reason could be attributed to the kinetic process because it was reported that CO_2 may require much longer time to react with sodium compounds while reaction rate of water with sodium seems very faster. That could explain why Na_2CO_3 was difficult to be identified by XRD analysis.

Secondly, mass transportation of water vapor may also strongly hamper its reaction with other compounds. The formation of NaOH may require much more amounts of H_2O than that the inlet system could supply as the gas inlet amount is limited to a molecular flow range to prevent the equilibriums inside the Knudsen cell from

destruction. For instance, the formation of 1 mg NaOH may require at least 7-14 hours in these gas-inlet experiments if 5-10% inlet H_2O reacted with Na-Fe oxides. For this reason, introduction of water vapor and CO_2 into the KC seems not enough to cause the corresponding reactions to a considerable extends in the gas-inlet KEMS experiments. If the reaction time is long enough, the calculated equilibrium states should be established finally.

Table 18: Experiment results of Na_5FeO_4 at various environmental conditions investigated by gas-inlet KEMS

Test sample	Gas inlet conditions	Gas pressure inside the K-cell	Observed compounds by XRD	Memo
Na_5FeO_4	H_2+CO_2 inlet 873-923K, 20hrs	P_{H2O}=0.5~1Pa P_{CO2}=0.5~1Pa P_{Na}=1~10Pa P_{NaOH}=10^{-2}~1Pa	Na_5FeO_4, $Na_8Fe_2O_7$, NaOH	No evidence of Na_2CO_3 and other Na-Fe oxides were found. Possible reaction: $2Na_5FeO_4+H_2O=Na_8Fe_2O_7+2NaOH$ $2Na_5FeO_4=Na_8Fe_2O_7+2Na+O_2$
Na_5FeO_4	CO_2 inlet 873-923K, 20hrs	P_{CO2}=0.5~1Pa P_{Na}=1~10Pa	Na_5FeO_4, $Na_8Fe_2O_7$	No evidence of Na_2CO_3 and other Na-Fe oxides were found. Thermal decomposition would have occurred. $2Na_5FeO_4=Na_8Fe_2O_7+2Na+O_2$
Na_3FeO_3	H_2+CO_2 inlet 873-923K, 20hrs	P_{H2O}=0.5~1Pa P_{CO2}=0.5~1Pa P_{Na}=1~10Pa P_{NaOH}=0.04-1Pa	Na_3FeO_3, $NaFeO_2$ NaOH Fe_3O_4,	No evidence of Na_2CO_3 and other Na-Fe oxides were found. Possible reaction: $Na_3FeO_3+H_2O=NaFeO_2+2NaOH$
Na_5FeO_4	H_2+O_2 inlet 523-573K, 10hrs, 53hrs, 108hrs.	P_{H2O}=8~10Pa P_{Na}<1E-3Pa	Na_5FeO_4, NaOH Na_3FeO_3 $NaFeO_2$	NaOH was found from the initial stage. When the amount of Na_5FeO_4 decreased, Na_3FeO_3 and $NaFeO_2$ were found. Possible reactions would be, $Na_5FeO_4+H_2O$. $Na_3FeO_3+2NaOH$ $Na_3FeO_3+H_2O$. $NaFeO_2+2NaOH$
Na_5FeO_4	CO_2 inlet 523-573K, 100hrs	P_{CO2}=8~10Pa P_{Na}<1E-3Pa	Na_5FeO_4	No evidence of Na_2CO_3 and other Na-Fe oxides were found. No reactions observed.

4.2.2 Experiment by massive gas-flow test

To overcome the shortcomings of the gas-inlet KEMS experiments, a separated experiment conducted by T. Furukawa [43] may provide another evidence to support the above conclusions, in which flowing air including water vapor and CO_2 was sweeping over $Fe+Na_2O_2$ at rate of 100ml/min at 823 K. In this condition, the gas amounts were about 120 times than that used in the gas-inlet KEMS experiments. The relationship between reaction time and the products was given in Table 19.

It showed that NaOH was formed since the very beginning. Na_2CO_3 was able to be identified by XRD after a few hours. It can also be noticed that the longer the reaction time, the more the content of Na_2CO_3. $NaFeO_2$ was found as the final stable sodium ferrite. At the initial stage, however, no sodium ferrites were found except for Fe_2O_3. It indicated that the Na_2CO_3 was probably formed via reaction of $NaOH+CO_2$, instead of reaction between sodium ferrites and CO_2 directly. The reason might be that the reaction speed of $NaOH+CO_2$ is much more faster. These results again suggested that reaction rate of CO_2 with sodium ferrates would be much slower than other possible reaction routes.

Table 19: $Fe+Na_2O_2$ in H_2O+CO_2 at 823 K

Time (hour)	Observed products
2	Na_2O_2, NaOH
4.5	Na_2O_2, NaOH, Fe_2O_3
7	NaOH, Na_2CO_3, $NaFeO_2$, Na_2O_2
20	$NaFeO_2$, Na_2CO_3, NaOH

* Products listed in order of its amount identified by the XPD analysis

4.2.3 Applications to corrosion analysis in case of the sodium-leak incident of FBRs

From early studies by Aoto[44] and Furukawa[45], two corrosion mechanisms were proposed, i.e., the corrosion by means of formation of Na-Fe complex oxides and the Molten Salts Corrosion. The corrosion rates in the later case were about several times faster than those in the former case. So, the later type of corrosion is of more significance for the safety analysis point of view.

The formation of NaOH was a necessary condition for the Molten Salts Corrosion. According to the previous calculation, it is clear that NaOH is thermodynamically stable as long as water vapor is present in the surrounding environment. The further experiments in various gas-inlet conditions again confirmed

that NaOH can be formed even if the water vapor pressure is very low. So, the Molten Salts Corrosion would happen in such a condition that the water vapor supply is adequate. Thus, water vapor transport from the surrounding area to the reaction zone will play important role in this process. Corrosion mechanisms at different location may be quite different depending on its local environmental conditions. For example, the reaction zone can be classified as the following two large types:

- The open interface of Fe and the reactants exposed to the atmosphere, where water vapor can be supplied from the air.

  In this zone, a quantity of NaOH liquid could be formed. If the environmental condition meets other requirements for occurrence of the Molten Salt Corrosion mechanism, a high corrosion rate to the iron-based structure materials could not be avoided. Since the corrosion speed is a few times higher than those in nearby areas, it consequently would result in holes in the steel and let sodium penetrate the steel to cause further serious damages. In theory, possibility of the contact of sodium with concrete flour could not be denied. However, the probability of explosion out of reaction of sodium with the water stored in the concrete is almost impossible, because the stored water in concrete can not meet the demand that an explosion requires in a instant moment.
- The close inner zone isolated by the reactant and products, where only very limited amount of water and carbon dioxide were enclosed in the reaction system.

  In these zones, Na-Fe complex oxides would be the main reaction products. The chemical states of sodium ferrates will be determined by temperature, oxygen potential and the amount of sodium. If the local oxygen had been consumed very quickly, the oxygen potential would decreased to such a low level that even Na_4FeO_3 would be stable. During the development of the whole complex chemical reaction processes, oxygen potential might also have chances to change by various oxygen transportation processes, such as diffusion through the liquid, solid or other tunnels formed during the Molten Salt Corrosion occurred in neighbors. So, formation of other sodium ferrites like Na_5FeO_4, Na_3FeO_3 as well as $NaFeO_2$ would be also reasonable. Considering the thermal decomposition of sodium ferrites at high temperatures, $NaFeO_2$ and Na_3FeO_3 would have higher probability to be found in these areas in case of the sodium-leak incident.

Summary and conclusions

The present study described research works on research and development of the gas-inlet high temperature mass spectrometer, experimental measurements of the Gibbs free energy of unknown Na-Fe oxides, evaluation of the thermodynamic functions in Na-Fe-O system, construction of user database for thermodynamic calculations, simulation calculation in Na-Fe-O-H-C system, creation of Na-Fe-O ternary phase diagrams and chemical potential diagrams in Na-Fe-O-H-C system, chemical stability of Na-Fe oxides in various environmental conditions, experiments on chemical states of Na-Fe oxides in H_2O/CO_2 environments, as well as the discussion of corrosion behaviors in various environmental conditions.

Based on the present studies, main conclusions are as the following:

- The sodium ferrites, $NaFeO_2$, Na_3FeO_3, and Na_5FeO_4 could be formed in a wide range of temperature, oxygen potential and sodium pressure, while Na_4FeO_3 could be stable only at low oxygen potentials. $Na_8Fe_2O_7$ and $Na_3Fe_5O_9$ were found as the high temperature phases but $Na_4Fe_6O_{11}$ might be a metastable phase and tend to decompose to other sodium ferrites like $NaFeO_2$. Na_2FeO_2 does not exist and $Na_{31}Fe_8O_{29}$ reported in some literatures actually should be $Na_8Fe_2O_7$. Other higher order sodium iron oxides with $Fe^{+4,+5,+6}$ are unstable and will decompose to lower oxidation states.

- The equilibrium states in Na-Fe-O-H-C is greatly depends on the environmental conditions. Apart from temperature, oxygen potential and sodium pressure, the water vapor pressure and carbon dioxide pressure also have strong influence on behaviors of Na-Fe oxides in the Na-Fe-O-H-C system.

- Molten salt NaOH has high possibility to be formed in a wide range of temperature and gases conditions, which is one of the important factors in the so-called "Molten Salt Corrosion Mechanism" of sodium-leak incident of FBRs.

- It seems that the influence from CO_2 surpasses that of H_2O to dominate the chemical potential diagram, i.e., CO_2 may have stronger influence on equilibrium states in Na-Fe-O-H-C system than H_2O does. However, the kinetics of these chemical reactions may requires long time in hour-scale and sufficient mass transportation of water vapor and/or carbon dioxide

from the surrounding environment to the reaction zone. The formation of NaOH is actually the dominant process instead of Na_2CO_3 in case of sodium ferrates in H_2O+CO_2 environments.

- The corrosion type at specific locations of reaction zone will be depends on local environmental conditions. Molten Salts Corrosion would happen in the open interface where water vapor supply is adequate. On the other hand, the formation of Na-Fe complex oxides would be the main process in the closed inner areas that is isolated from the atmosphere by the reactants and products.

Acknowledgements

First, I gratefully acknowledge JNC to provide financial and technical support for this research project. It is my glory to propose this project, to make it stated, and see it completed as planed 3 years before. During the 3 years, I got a lot of supports and encouragements from the managers and directors of Oarai Engineering Center.

The Group leader Mr. Kazumi Aoto gave me such a free space that I could explore almost anything that is necessary for this research. Sometimes, the research topic went a little far away from nuclear application but much more close to fundamental researches. For example, I am very happy that theoretic study on electro impact ionization cross-sections could be carried out in JNC because its result is very significant for researchers in majors of High Temperature Mass Spectrometry.

I spend very happy time with my colleagues. Mr. Tomohiro Furukawa is in charge of the research coordination in the whole 3 years. His passion expanded the help from research aspects into my daily life. Mr. Kazuyuki Okubo did all the XRD analysis for my samples. His careful work guaranteed us to obtain reliable results from the experiments.

Finally, I do wish the research work introduced in this report would make some contribution to the safe construction and operation of the Monju FBR.

Thanks a lot !

References

[1] J. P. Coughlin, E. G. King, and K. R. Bonnickson, "High-temperature Heat Contents of Ferrous Oxide, Magnetite and Ferric Oxide", J. Am. Chem. Soc., Vol. 73, 1951, p3891-3893.

[2] Koehler M.F., Barany R. and Kelley K.K., "Heats and Free Energies of Formation of Ferrites and Aluminates of Calcium, Magnesium, Sodium and Lithium", U.S. Dept. of the Interior, Bureau of Mines 1961.

[3] Hiroshi Watanabe, "Weak Ferromagnetism in β–$NaFeO_2$", J. Phys. Soc. Jpn., Vol.16, No. 6, p1181-1184, 1961.

[4] W. Dai, S. Seetharaman and L.-I. Staffansson, Scand. J. Metall., Vol.13, p32-38, 1984.

[5] W. Dai, S. Seetharaman and L.-I. Staffansson, "Phase-Relationships in the System Fe-Na-O", Metallurgical Transactions, Vol. 15B, p319-327, 1984.

[6] S. Seetharaman and Du S., "An evaluation of the Stabilities of the Ternary Compounds at Low Oxygen Potentials in the Ternary System Fe-Na-O", High Temperature Materials and Processes, Vol. 12, No. 3, p145-153, 1993.

[7] M. Yamawaki, F. Ono et al., JNC report, TY9400 2001-006, 2000.

[8] D. D. Wagman et al., The NBS Tables of Chemical Thermodynamic Properties, National Bureau of Standarda, Washingto, D.C. [J. Phys. Chem. Ref. Data, Vol. 11, 1982, Suppl. No.2].

[9] Ihsan Barin, "Thermochemical Data of Pure Substances", Vol. 1, p708, VCH publishers, New York 1995.

[10] T. Lindemer and T. M. Besmann, "Thermodynamic Review and Calculations: Alkali-metal oxides systems with nuclear fuels, fission products, and structural materials", J. Nucl. Mater., 100(1981)178-226.

[11] KTH, Thermo-Calc compatible Fe-Na-O-H database, private communications.

[12] H. Yokokawa, N. Sakai, T. Kawada and M. Dokiya, "Estimated and evaluated values during 1989-1991", J. Solid State Chem., Vol. 94, p106-120, 1991.

[13] R. Sridharan, D. Krishnamurthy and C.K. Mathews, "Thermodynamic Properties of Ternary Oxides of Alkali Metals from Oxygen Potential Measurements", J. Nucl. Mat., Vol. 167, p265-270, 1989.

[14] N.P. Bhat and H.U. Borgstedt, "Thermodynamic Stability of Na_4FeO_3 and Threshold Oxygen Levels in Sodium for the Formation of This Compound o AISI 316 Stell Surfaces", J. Nucl. Mat., Vol. 158, 1988.

[15] B.J. Shaiu, P.C.S. Wu and P. Chiotti, "Thermodynamic Properties of the Double oxides of Na_2O with the Oxides of Cr, Ni and Fe", J. Nucl. Mat., Vol. 67, p12-23,

1977.

[16]R. Sridharan, T. Gnanasekaran and C. K. Mathews, "Phase Equilibrium Studies in the Na-Fe-O System", J. Alloys & Compounds, Vol. 191, p9-13, 1993.

[17]R. Sridharan, T. Gnanasekaran, G. Periaswami and C. K. Mathews, "Thermochemistry of Na-Fe-O System and its Relevance to Corrosion of Steels in Sodium", Liquid Metal Systems, p269-277, edited by J. Borgstedt and G. Fress, Plenum Press, New York, 1995.

[18]Jeannot C., Malaman B., Gérardin R. and Oulladiaf B., "Synthesis, Crystal, and Magnetic Structures of the Sodium Ferrate(IV) Na_4FeO_4 Studied by Neutron Diffraction and Mössbauer Techniques", J. Solid State Chem., 165(2002)266-277.

[19]Dedushenko S. K., Kholodkovskaya L. N., et al., "On the possible existence of unusual higher oxidation states of iron in the Na-fe-O system", J. Alloys Compounds, 262-263(1997)78-80.

[20]Jintao Huang, T. Furukawa and K. Aoto, JNC report TN9400 2000-101, "System Assessment and Calibrations of the Knudsen Effusion Quadrupole Mass Spectrometer", Aug. 2000.

[21]Jintao Huang, T. Furukawa and K. Aoto, JNC report ,JNC TN9400 2002-069, "Physical and Chemical Properties of sodium ferrates and equilibrium calculations in H_2O/CO_2 environment", Jan. 2003.

[22]Jintao Huang, T. Furukawa and K. Aoto, "Thermodynamic study of sodium-iron oxides Part I: Mass spectrometric study of Na-Fe oxides", Thermochimica Acta, 2003 (in print).

[23]Klaus Hilpert, "Chemistry of Inorganic Vapors", Structure and Bonding 73, p97-198, Springer-verlag Berlin Heidelberg 1990.

[24]Jintao Huang, Doctoral Thesis, No. tt47282, Department of Quantum Engineering & System Science, the University of Tokyo, Sept. 30, 1997.

[25]Jintao Huang, T. Furukawa and K. Aoto, JNC report TN9400 2001-095, "Determination of Gibbs Energy of Formation of Na_3FeO_3 by High Temperature Mass Spectrometer", Oct. 2001.

[26]L.N. Gorokhov, A.M.Emel'yanov and I.V.Sidorova, "Vapor composition and the Thermodynamics of vaporization of sodium hydroxide", Russian J. Phys. Chem, Vol.70, No.6, 1996,p930-933.

[27]J. Huang, T. Furukawa, K. Aoto and M. Yamawaki, J. Mass Spectrometry Society of Japan, "Study of electron impact ionization cross-sections of sodium-containing molecules", Vol.50, No.6, 2003, p296-300.

[28]Jintao Huang, JNC report TN9400 2001-046, "Quantum Mechanic Study of Electron Impact Ionization Cross Sections of Sodium-containing Molecules", Feb. 2001.

[29]J. K. Fink and L. Leibowitz, "A Consistent Assessment of the Thermophysical Properties of Sodium", High Temperature and Materials Science, Vol.35, 65-103

1996, (Argonne National Laboratory Report, ANL/RE-95/2, 1995).

[30]Malcolm W. Chase, Jr., "NIST-JANAF Thermochemical Tables Fourth Edition", J. Phys. Chem. Ref. Data, Monograph No.9.

[31]B. Sundman, B.Jansson and J.-O.Andersson, Calphad 9(1985)153.

[32]H. Yokokawa, S. Yamauchi and T. Matsumoto, Themochimica Acta, 245 (1994) 45.

[33]Robert Collongues et Jeanine Thery, "Préparation et propriétés des ferrites de sodium", Bull. Soc. Chim France, No. 186(1959)1141-1144.

[34]Watanabe H. and Fukase M., "Weak ferromagnetism in β-$NaFeO_2$", J. Phys. Soc. Jpn., 16(1961)1181-1184.

[35]Hua Shounan, Cao Gaoping and, Cui Yuezhi, "Sodium ferrite $Na_2O{\cdot}1.5Fe_2O_3$ as a high-capacity negative electrode for lithium-ion batteries", J. Power Sources, 76(1998)112-115.

[36]Orient O. J. and Srivastava S. K.,"Electron impact ionisation of H_2O, CO, CO_2 and CH_4" J.Phys. : Atomic, molecular and optical physics, Vol.20, issue15, p3923-3936, 1987.

[37]Freund R. S., Wetzel R. C., Shul R. J. and Hayes T. R., "Cross-section measurements for electron-impact ionization of atoms", Phys. Rev., A 41(1990) 3575-3595.

[38]T.B. Massalski, Binary Alloy Phase Diagram, 2nd edition, 1990, ASM International.

[39]P. Gross and G.L. Wilson, J. Chem. Soc. A, (1970)1913.

[40]J.M. Stuve, L.B. Pankratz and D.W. Richardson, US Department of the Interior, Bureau of Mines, Report of investigations 7535, 1971.

[41]Kale G. M. and Srikanth S., "Electrochemical determination of the Gibbs energy of formation of $Na_2Fe_2O_4$ and $Na_3Fe_5O_9$ employing Na-β-Al_2O_3 solid electrolyte", J. Am. Ceram. Soc., 83(2000)175-180.

[42]Knights C.F. and Phillips B.A., "Phase diagrams and Thermodynamic studies of the Cs-Cr-O, Na-Cr-O and Na-Fe-O systems and their relationships to the corrosion of steels by caesium and sodium", High Temperature Chemistry of Inorganic and Ceramic Materials, p134-145, ed. Glasser F.P. and Potter P.E., The Chemical Industry:London, 1977.

[43]Tomohiro, Furukawa, JNC report ,JNC TN9400 2002-071.

[44]K. Aoto, "Corrosion Mechanism of Mild Steel in Buring Sodium and its Compounds", High Temperature Corrosion and Materials Chemistry, ed. by P.Y. Hou, et.al., the Electrochemical Society, Inc., p287-298, 1998.

[45]T. Furukawa, E. Yoshida, Y. Nagae and K. Aoto, "The High Temperature Chemical Reaction between Sodium Oxide and Carbon Steel", High Temperature Corrosion and Materials Chemistry, ed. by P.Y. Hou, et.al., the Electrochemical Society, Inc., p2312-423, 1998.

[46]Huang Jintao, Furukawa Tomohiro and Aoto Kazumi, "Thermodynamic study of sodium-iron oxides Part II: Ternary phase diagram of the Na-Fe-O system",

Thermochimica Acta, 2003(in print).

[47]Huang Jintao, Furukawa Tomohiro and Aoto Kazumi, "High temperature behavior of Na-Fe oxides in H_2O+CO_2 atmosphere", (accepted to present in the 11th International IUPAC Conference on High Temperature Materials Chemistry, Tokyo, May 19-23, 2003, to be published Journal of Physics and Chemistry of Solids).